Bio-functionalization of microcarriers for the expansion of human neural stem cells

Cheila Patrícia de Oliveira Madaleno

Thesis to obtain the Master of Science Degree in

Biomedical Engineering

Supervisors: Dr. Carlos André Vitorino Rodrigues

Prof. Frederico Castelo Alves Ferreira

Examination Committee

Chairperson: Prof. Ana Luísa Nobre Fred

Supervisor: Dr. Carlos André Vitorino Rodrigues

Members of the Committee: Prof. Maria Margarida Fonseca Rodrigues Diogo

December 2015

Acknowledgments

I would like to acknowledge Professor Margarida Diogo for proposing my name for this thesis. A special thanks to Professor Joaquim Sampaio Cabral for giving me the opportunity to work in the SCBL-RM.

I am deeply grateful to Dr. Carlos Rodrigues, for his guidance, patience, and teaching. I will never forget the answer to every question: 'Agitar!'.

I would like to thank also to prof. Frederico Ferreira for the support and to be available to discuss the work.

A special thanks for all the members of SCBL which helped me throughout my work, particularly to Miriam Sousa and Marta Costa, and to Teresa Esteves and Ana Vicente who kindly explained to me the infrared spectroscopy.

To all my colleagues of the master´s room: André Silva, Joana Pinho and Francisco Pinheiro,

To all my friends who were and are still present.

Mais importante ainda, quero agradecer aos meus pais, ao meu irmão e à minha família todo apoio que me deram durante o meu percurso, principalmente nestes últimos 5 anos que foram dos mais difíceis e desafiantes da minha curta vida, ainda assim dos mais felizes. Espero que se sintam tão orgulhosos de mim quanto eu me sinto de vocês.

Um grande OBRIGADO!

Abstract

The need to provide an unlimited supply of neural stem cells (NSCs) for scientific research and clinical applications is the drive for the development of efficient large scale bioprocesses. Microcarriers, which provide a surface for cell adhesion in suspension, combined with bioreactors are a possible scalable strategy. There are several microcarriers commercially available, however, there is a great need to design microcarriers tailored for the expansion of specific stem cell lines. This work focused on the functionalization of microcarriers' surface to enhance attachment and proliferation of long- term neural stem cell (lt-NES), when cultured under dynamic conditions. A screening of microcarriers improved by surface conjugation using two different techniques, laminin covalently bond through a 1-ethyl-3-[3-dimethylaminopropyl]carbodiimide (EDC) and N-hydroxysuccinimide (NHS) based reaction or through passive adsorption, was performed in static conditions. On the basis of those results, poly-ornithine/laminin adsorbed Plastic and laminin crosslinked Carboxyl microcarriers were compared in a spinner flask culture. Carboxyl microcarriers supported lt-NES proliferation in static conditions but cell detachment was observed in spinner flask. Plastic microcarriers revealed to be more efficient in lt-NES culture in a spinner flask, reaching a maximum fold increase of 1.69. Moreover, maintenance of lt-NES phenotypic properties expanded in the latter approach was verified by expression of neural markers Nestin and Sox2. The results obtained may be the basis for future optimizations of culture parameters for lt-NES expansion.

Keywords: Microcarriers; Neural Stem Cells; EDC-sulfo NHS reaction; Adsorption;

Resumo

A necessidade de estabelecer uma fonte ilimitada de células estaminais neurais para aplicação em investigação científica e em terapias clínicas é a base para o desenvolvimento de bioprocessos eficientes de larga escala. O uso de micropartículas, que proporcionam uma superfície para as células aderirem em suspensão, em conjunto com bioreactores é uma possível estratégia. Existem várias micropartículas disponíveis comercialmente, no entanto, ainda existe uma grande necessidade de desenvolver micropartículas adequadas à expansão de linhas celulares específicas. Este trabalho centrou-se na funcionalização da superfície das micropartículas para melhorar a adesão e proliferação de uma linha particular de células estaminais neurais (lt-NES), quando cultivadas em condições dinâmicas. Micropartículas funcionalizadas com laminina, quer através de uma reacção de ligação covalente (EDC/NHS) quer por adsorção passiva, foram comparadas em condições estáticas. Com base nos resultados obtidos, as micropartículas adsorvidas ou ligadas covalentemente à laminina foram testadas em sistemas agitados (spinner flasks). As partículas conjugadas covalentemente com laminina promoveram a adesão e o crescimento celulares em condições estáticas, mas resultados semelhantes não foram observados no spinner flask. As partículas adsorvidas com laminina revelaram ser mais eficientes na cultura das lt-NES em sistema agitado, resultando num *fold increase* de 1.5. Além disso, verificou-se a manutenção das propriedades fenotípicas das lt-NES expandidas nesse último sistema de cultura, através da expressão de marcadores neuronais tais como a Nestina e o Sox2. Os resultados obtidos neste trabalho poderão servir de base a futuras optimizações dos parâmetros de cultura para a expansão de lt-NES.

Palavras-chave: Micropartículas; Células Estaminais Neurais; Reacção EDC/sulfo-NHS; Adsorpção

Contents

1 INTRODUCTION 1

1.1 STEM CELLS 1
1.1.1 Embryonic Stem Cells 1
1.1.2 Induced Pluripotent Stem Cells 1
1.1.3 Neural Stem Cells 2
1.1.3.1 *In vivo* sources of NSCs 2
1.1.3.2 NSCs *in vitro* derivation 3
1.1.3.3 NSCs Culture 5
1.1.3.4 Applications of NSCs 6
1.2 SCALE-UP CULTURE STRATEGIES 7
1.2.1 Bioreactor systems for stem cell culture 7
1.2.2 3D culture systems 10
1.2.2.1 Cell aggregates 11
1.2.2.2 Cell encapsulation 11
1.3 MICROCARRIERS 12
1.3.1 Microcarriers properties 12
1.3.2 Adhesion to microcarriers 14
1.3.3 Materials and surface properties 14
1.3.4 Surface Functionalization 15
1.3.4.1 EDC/sulfo-NHS coupling 16
1.3.4.2 Coating substrates and molecules 17
1.4 SCALE-UP STRATEGIES FOR NSC 18
1.5 AIM AND MOTIVATION OF STUDIES 20
1.6 NOVELTY 21

2 MATERIALS AND METHODS 22

2.1 MICROCARRIERS PREPARATION AND BIO-FUNCTIONALIZATION 22
2.1.1 Surface functionalization via EDC/NHS crosslinking 23
2.1.2 Surface functionalization through adsorption 24
2.2 CROSSLINKING REACTION VALIDATION USING THE BRADFORD ASSAY 24
2.3 LT-NES CELL CULTURE 24
2.3.1 Lt-NES cell thawing 25
2.3.2 Lt-NES cell passaging 25
2.3.3 Lt-NES cell freezing 25
2.3.4 Lt-NES cell expansion on microcarriers under static conditions 26
2.3.5 Lt-NES cell expansion on microcarriers under dynamic conditions 26
2.3.5.1 Analysis of metabolites and nutrients in culture medium 27
2.4 LT-NES CELL CHARACTERIZATION 27
2.4.1 Immunocytochemistry 27
2.5 STATISTICAL ANALYSIS 28

3 RESULTS AND DISCUSSION 29

3.1 VALIDATION OF THE EDC/SULFO-NHS CROSSLINKING IN SURFACE CONJUGATION 29
3.2 LT-NES CELL CULTURE UNDER STATIC CONDITIONS 32
3.2.1 Comparison of adsorbed and crosslinked microcarriers 39
3.3 LT-NES CELL CULTURE UNDER DYNAMIC CONDITIONS 42
3.3.1 Caboxyl microcarrier culture in spinner flask 42

3.3.2 Plastic microcarrier culture in spinner flask 45

4 CONCLUSIONS 51

5 REFERENCES 53

List of Figures

Figure 1: Niches of NSCs in the rat brain. Adapted from (Crews and Nixon 2003) 3
Figure 2: Sources of NSCs (Adapted from (Conti and Cattaneo 2010)) 4
Figure 3: NSCs in vitro culture systems and outcomes of neuronal differentiation. Adapted from (Conti and Cattaneo 2010). 6
Figure 4: Several bioreactor configurations. a) Roller botlles; b) Stirred tank; c) Spinner flasks (Adapted from (Scientific , Cabrita, Ferreira et al. 2003)) 8
Figure 5: Several bioreactor configurations. a) Air lift ; b) Wave bioreactor; c) Hollow-fiber; d) Fixed or fluidized bed; e) Rotating-wall vessel. Adapted from (1999, Cabrita, Ferreira et al. 2003, Barzegari and Saei 2012) 10
Figure 6: Representation of 3D culture systems. a) cell aggregates; b) Microcarriers; c) Encapsulated cells; Adapted from (Serra, Brito et al. 2012) 11
Figure 7: EDC/sulfo-NHS coupling reaction scheme. (1) and (2) can be proteins, peptides or chemicals containing carboxyl or primary amine groups, respectively (Scientific) 17
Figure 8: Laminin structure. Chains A, B1 and B2 each containing the NH_2 terminus. 1) ECM assembly; 2) triple coiled-coil represented by parallel straight lines; 3) cell-surface receptor binding domain; 4) collagen binding domain. Adapted from (Beck, Hunter et al. 1990) 18
Figure 9: Schematics of EDC/sulfo-NHS mediated covalent attachment of laminin on the surface of carboxyl polystyrene beads. 23
Figure 10: Absorbance of supernatant samples of laminin crosslinked beads, measured right before and after the incubation period of the reaction. Absorbance of uncoated beads (blank) and laminin adsorbed beads were measured at the same time periods. Results of crosslinking are the average of 3 independent experiments, uncoated and adsorption are the average of 2 independent experiments. Error bars represent SEM 30
Figure 11: Laminin calibration curve 30
Figure 12: Comparison of BSA and laminin standard curves 32
Figure 13: lt-NES culture in day 5, under static conditions, in uncoated microcarriers (A,D,F), poly-ornithine coated microcarriers (B), poly-ornithine/laminin coated microcarriers (C) and laminin crosslinked microcarriers (E,G) 34
Figure 14: lt-NES culture in day 5, under static conditions, in uncoated (A,C) and poly-ornithine/laminin coated Cytodex 1 and Cytodex 3 (B,D) 35
Figure 15: Cell number and fold expansion after 6 days of culture in Plastic, Cytodex 1 and –COOH beads under static conditions. PO: poly-ornithine; LN: laminin. Results of one experiment 36
Figure 16: lt-NES harvested from laminin conjugated carboxyl (A), poly-ornithine/laminin adsorbed Cytodex 1 (B) and Plastic (C) microcarriers and replated in poly-ornithine/laminin tissue culture plates 37
Figure 17: Immunostaining of cells for NSC markers Nestin (A-C), Sox 2 (D-F) and neuronal differentiation marker Tuj1 (G-I) expression after culture in poly-ornithine/laminin adsorbed Plastic microcarriers under static conditions. 37
Figure 18: Immunostaining of cells for NSC markers Nestin (A-C), Sox 2 (D-F) and neuronal differentiation marker Tuj1(G-I) expression after culture in laminin conjugated –COOH microcarriers under static conditions. 38

Figure 19: Immunostaining of cells for NSC markers Nestin (A-C), Sox 2 (D-F) and neuronal differentiation marker Tuj1 (G-I) expression after Cytodex 1 culture under static conditions. 38
Figure 20: Cell numbers after 6 days of culture in adsorbed Plastic and Cytodex 1 beads and conjugated -COOH beads, with different laminin concentrations. Results of one experiment 40
Figure 21: Bead aggregation evolution under static conditions in poly-ornithine + laminin 3µg/cm^2 Plastic, Cytodex 1 beads and, laminin 3µg/cm^2 Carboxyl 41
Figure 22: Bead aggregation evolution under static conditions in laminin 2µg/cm^2 Carboxyl microcarriers 42
Figure 23: Growth curve of lt-NES cultured in spinner flasks with 3µg/cm^2 laminin crosslinked –COOH beads. Results of one experiment 43
Figure 24: lt-NES cell occupancy on –COOH beads harvested in day 1, 3 and day 5 of culture in spinner flask. 43
Figure 25: Concentration profile of glucose (■) and lactate (●), in mM, during lt-NES -COOH beads culture in spinner flask. Results of one experiment 44
Figure 26: Growth curve of lt-NES cultured in spinner flasks with 3µg/cm^2 laminin coated plastic beads. Results of one experiment 46
Figure 27: Cell density over time (days). Initial surface area available was 108 cm^2, increased in day 5 to 180 cm^2. Results of one experiment 46
Figure 28: lt-NES cell occupancy on Plastic beads harvested in days 1, 3, 5, 7, 9 and 10 of culture in spinner flask 47
Figure 29: Immunostaining of cells for NSC markers Nestin (A-C), Sox 2 (D-F) and neuronal differentiation marker Tuj1 (G-I) expression in plastic beads cultured in spinner flasks. 48
Figure 30: Immunostaining of cells harvested from plastic beads cultured in spinner flasks and replated in poly-onithine/laminin tissue culture plates. Evaluation of NSC markers Nestin (A-C), Sox 2 (D-F) and neuronal differentiation marker Tuj1(G-I) expression 48
Figure 31: Concentration profile of glucose (■) and lactate (●), in mM, during lt-NES plastic beads culture in spinner flask. Results of one experiment 49

List of Tables

Table 1: Characteristics of some commercially available microcarriers. 13
Table 2: Properties of the microcarriers used in this work. Note: * cm^2/ dry weight. 22
Table 3: Primary antibodies and respective dilutions used in immunochemistry assays. 28
Table 4: Secondary antibody used in immunocytochemistry assays. 28
Table 5: Laminin **c**oncentration and mass present in the supernatant samples of crosslinked beads and coupled through adsorption, and protein attachment efficiency of the respective coating procedures. Initial: Before the incubation period; Final: after the incubation period 31
Table 6: Qualitative assessment of attachment and survival of cells, occurrence of free cell aggregates in the medium and bead aggregation due to cell "bridging" in the different types of coated microcarriers and respective controls 33
Table 7: Growth parameters of lt-NES cultured in spinner, adherent to plastic beads. Fold expansion relates to to expansion of inoculated cells, adherent cell fold expansion relates to the expansion of adherent cells, at day 1. Maximum fold expansion relates to the best cell culture day 45
Table 8: Average specific glucose consumption (q_{glu}), specific lactate production (q_{lac}) and average molar ratio of lactate produced over glucose consumption in different time periods of Plastic microcarrier in spinner flask culture. 50

List of Abreviations

2D – Two Dimensional

3D – Three -Dimensional

AMD - age-related macular degeneration

APMAAm - aminopropylmethacrylamide

BPs - Basal Progenitors

BSA – Bovine Serum Albumine

CNS – Central Nervous System

DAPI – 4',6-Diamino-2-Phenylindole dilactate

DEAE - Diethylaminoethyl

DMEM – Dulbecco's Modified Eagle´s Medium

DMSO - Dimethyl Sulfoxide

EB - Embryoid Bodies

ECM - Extracellular Matrix

EDC - 1-ethyl-3-(3-dimethylaminopropyl) Carbodiimide

EGF - Epidermal Growth Factor

ESCs – Embryonic Stem Cells

FGF-2 – Fibroblast Growth Factor

GFAP - Glial Fibrillary Acid Protein

GMP – Good Manufacturing Practices

hESCs – Human Embryonic Stem Cells

iPSCs - Induced Pluripotent Stem Cells

lt-NES - Long-term Neural Stem Cell

MES - 2-[morpholino]ethanesulfonic Acid

NEPs – Neuroepithelial Progenitors

NHS - N-hydroxysuccinimide

Sulfo-NHS - N-hydroxy Sulfosuccinimide

NSCs – Neural Stem Cells

PBS –Phosphate Buffered Saline

pLL – Polylysine

PMEDSAH - poly[2-(methacryloyloxy)ethyl dimethyl-(3-sulfopropyl)ammonium hydroxide]

PSCs – Pluripotent Stem Cells

RG – Radia Glial

RGD - Arginine-Glycine -Aspartic Acid

SEM – Standard Error of the Mean

SGZ - Subgranular Zone

SVZ - Subventricular Zone

TUJ1 - βIII-tubulin

UV – Ultra-Violet

1 Introduction

1.1 Stem Cells

Stem cells emerged as a promising tool for research and therapeutic applications. Their unique features, the long-term capacity to generate identical stem cells (self-renewal) indefinitely and the ability to differentiate into other cells with specialized functions (potency), have brought new perspectives in the fields of regenerative medicine, drug discovery and disease modeling.

To this date, various types of stem cells have been isolated and identified from different sources of the organism, in different stages of potency and are classified according to their potential to differentiate. Stem cells can be totipotent if they are capable of generating a whole organism. An example is the zygote (fertilized ovum). When a stem cell can generate cells from the three embryonic germ layers (ectoderm, endoderm and mesoderm) but lack the capacity to form an entire organism they can be classified as pluripotent stem cells (PSCs). Moreover, multipotent cells can differentiate into various cell types present in a specific tissue or organ and unipotent cells are able to give rise to a single cell type [1].

1.1.1 Embryonic Stem Cells

Embryonic stem cells (ESCs) are pluripotent stem cells derived from embryos. ESCs are isolated from the inner cell mass of the blastocyst (a 5-day embryo) and cultured *in vitro*. They are capable of proliferating indefinitely while maintaining their undifferentiated state [2].

In 1998, the generation of the first ESC line derived from human embryos was reported by Thomson *et al* [3]. These cells, termed human embryonic stem cells (hESCs), express certain genes essential for the maintenance of the undifferentiated, pluripotent state, namely Oct4, Nanog, and Sox2. Several other factors were also identified as markers of hESCs, such as the surface markers Tra-1-60, Tra-1-81, SSEA-3, SSEA-4 and alkaline phosphatase [2, 3]. Despite their clinical relevance, hESCs face ethical concerns regarding the use of human embryos for their derivation, and safety issues due to possible immune reactions after transplantation. Furthermore, establishment of robust protocols for differentiation into the desired target cells and/or efficient purification methods are essential to prevent the formation of teratomas after transplantation.

1.1.2 Induced Pluripotent Stem Cells

In 2006, Shynia Yamanaka and his group reported the conversion of mouse fibroblasts into pluripotent stem cells using four transcription factors (Klf4, Sox2, Oct 3/4 and c-Myc), in a process called

reprogramming [4]. Those cells were named induced pluripotent stem cells (iPSCs). In the following year, the same author reported the generation of iPSCs from human somatic cells using the same transcription factors [5].

iPSCs represent a breakthrough discovery in the stem cell field since they resemble ESCs in their ability to proliferate without limit while maintaining the capacity to differentiate into all cell types of the three germ layers *in vitro*. Moreover, iPSCs avoid the ethical concerns of using human embryos and the problem of immune rejection since they can be derived directly from the patient. Despite their promising potential, iPSCs still have to overcome various obstacles in order to be a valuable therapeutic tool. The reprogramming process, for example, is far away from being optimized, and improvements such as increased efficiency and safety, as well as cost and time reduction are of great need. In addition, tumorigenecity of iPSC is a currently studied topic, since there are recent evidences that iPSCs are more prone to form teratomas, given the genetic modifications that occur during the reprogramming step and the possible retaining of the epigenetic memory of the cell of origin [6].

1.1.3 Neural Stem Cells

Neural stem cells (NSCs) are defined as multipotent cells and therefore, are able to self-renew for long periods of time and generate more restricted neural lineages, such as neurons and glia (including oligodendrocytes and astrocytes) [7]. These cells are present in the developing embryonic brain and, more recently, were identified also in certain regions of the adult brain where they might be able to regenerate diseased or injured sites [8].

1.1.3.1 *In vivo* sources of NSCs

Depending on the stage of CNS development and spatial organization, NSCs exhibit several morphologies and are present in different quantities. From neuroepithelium induction until CNS full maturation, NSCs undergo progressive restriction in their potency and self-renewal [9]. The origin of the central nervous system (CNS) begins with the induction of the neuroectoderm which forms the neural plate and, later, the neural tube, structures where neuroepithelial progenitors (NEPs) can be identified.

Radial glia (RG) is derived from NEPs at the beginning of neurogenesis and gradually replace the progenitors. RGs express typical astroglial markers and are a heterogeneous population of neural progenitors committed to different neural fates [10] . RG are involved in the migration of neurons towards their final destinations, provide structural support during axon growth, and probably are the source of multipotent adult neural stem cells[11]. From the asymmetric divisions of NEPs and RG result the basal progenitors (BPs), which reside in the subventricular zone (SVZ) in the developing telencephalon. This type of progenitors are associated with increased neuron production by undergoing symmetric cell

divisions that generate two neuronal daughter cells, explaining their alternative denomination of intermediate progenitors [12].

It was assumed that neurogenesis ceased in adulthood but there is now evidence that NSCs are still active in the adult mammalian brain, explaining its potential, although limited, to generate new neurons and glia. The so called adult progenitors reside in certain microenvironments called neurogenic niches (*Figure 1*), where conditions are favorable for the emergence of new neurons and preservation of self-renewal. The subgranular zone (SGZ) of the dentate gyrus of the hippocampus and the SVZ of lateral ventricles have been identified as neurogenic niches [9]. This finding reveals the residual plasticity of the brain, yet important for the replacement or repair of damaged neurons, in the learning process or memory. Given their potential role in adult life, the decline of NSCs proliferation with aging is a topic which needs further investigation. Also, the fact that NSCs are present only in restricted areas of the brain in small numbers and the difficulty to maintain them *in vitro* for multiple passages represent challenges regarding their isolation and expansion.

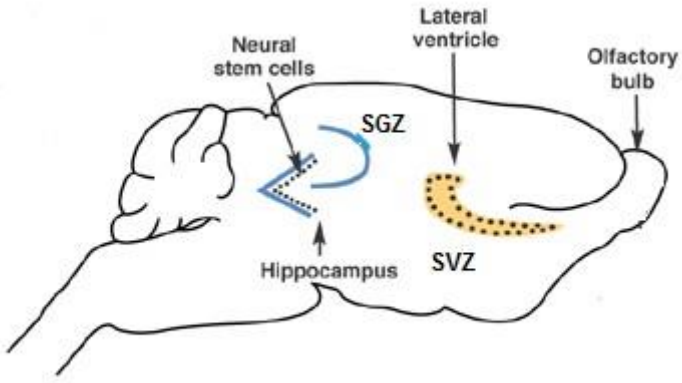

Figure 1: Niches of NSCs in the rat brain. Adapted from [13].

1.1.3.2 NSCs *in vitro* derivation

Neurodevelopment is a highly complex set of processes yet not completely understood. The mechanisms that trigger cells toward a neural fate are not characterized in detail; can either be removal of inhibitory factors, exposure to specific pathways, and are likely influenced by spatiotemporal dynamics of the developing brain. Nonetheless, researchers have been able to generate and propagate *in vitro* NSCs from ESCs or iPSCs differentiation, or to isolate and expand NSCs derived from the fetal or adult brain (*Figure 2*). Derivation of neural lineages from PSCs has been achieved with different protocols: embryoid body formation, co-culture with stromal cells, among others [2, 9, 14].

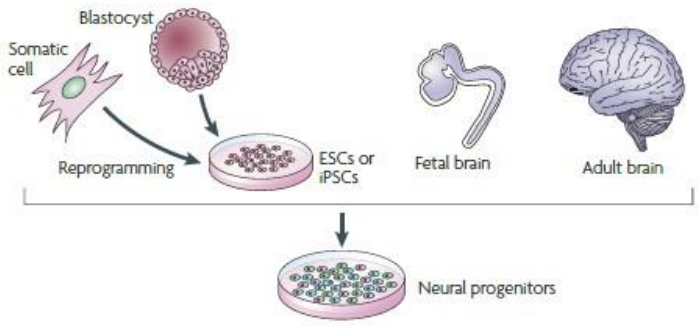

Figure 2: Sources of NSCs (Adapted from [7])

Embryoid bodies (EB) are spherical cell clusters observed after spontaneous or induced differentiation of PSCs cultured in low attachment plates. Induced differentiation can be promoted in EB by adding certain morphogens or growth factors. On the other hand, differentiation can be induced by direct cell-to-cell interactions between ESCs and other different cell types, in co-cultures systems. Several stromal cell lines are capable of inducing neural differentiation in co-cultures with ESCs and are typically isolated from the bone marrow [15]. Ideally, differentiation of PSCs into neuronal lineages would be performed in animal and feeder-free conditions, to avoid the risk of contamination with non-neural cells, using chemically defined medium and without EB formation, given their heterogeneity and gradients of nutrients, oxygen, etc [14].

Koch *et al*, generated and described a pure neural cell population termed long-term self-renewing neuroepithelial-like stem cell (lt-NES), which was the cell population used in this work [16, 17]. Briefly, the protocol for neural differentiation included hESC culture in suspension as EB, formation of neural rosettes, subsequent growth into three dimensions and manual isolation. The isolated structures were kept as floating spheres, dissociated into single cells and plated as a monolayer in poly-ornithine/laminin coated dishes in basal media enriched with N2 supplement, and in the presence of fibroblast growth factor (FGF-2), epidermal growth factor (EGF) and the B27 supplement [16, 17]. Lt-NES are capable of self-renewing for more than 100 passages while maintaining a stable potential for neurogenesis and glial differentiation. They express the neural precursor cell markers Nestin and Sox2, the neuronal progenitor transcription factors Sox1 and Pax6 and exhibit rosette patterns, which are typical of neural stem cells [16]. They are negative for the expression of neuronal and glial differentiation markers, βIII-tubulin (Tuj1) and Glial Fibrillary Acid Protein (GFAP), respectively. Lt-NES have been successfully derived both from hESCs and iPSCs [16], with the capacity to differentiate predominantly into GABAergic neurons, nonetheless, their differentiation ability can still be controlled towards different neuronal phenotypes using defined morphogens [17].

1.1.3.3 NSCs Culture

In the last decades, the NSCs field has benefited from the progresses achieved in cell isolation, purification and culture. NSCs can be expanded *in vitro* through adherent culture systems or as free-floating aggregates, termed neurospheres (*Figure 3*).

Neurospheres can be established in two ways: NSCs isolated from the fetal or adult brain or by ESCs/iPSCs derivation. NSCs isolated from adult and developing nervous system of rat and mice are dissociated into single-cell suspensions and then plated in defined serum-free media supplemented with EGF and FGF-2. These factors are vital to prevent spontaneous differentiation and to maintain self-renewal. However, neurospheres are characterized by their heterogeneity, containing cells in different stages of differentiation, and also by their low numbers of NSCs [7, 18]. The outcome of neurosphere systems is dependent on cell density, medium composition and culture methods (method and frequency of passaging, for example) [9]. A main weakness is the limitation of oxygen and nutrients diffusion in the center of the aggregate where accumulation of by-products tends to occur. As a consequence, neurospheres present a large variation within and between cultures, which makes it difficult for data comparison and interpretation [19]. It was believed that the 3-dimensional (3D) structure of this system could mimic the *in vivo* niches of NSCs, being a more relevant physiological model to study. Nonetheless, cells are growing in an *ex vivo* environment, lacking the characteristic spatial organization of the CNS, the specific cell-cell interactions with the neighborhood and exposure to biological molecules [7]. Although useful as a functional assay for NSCs, neurospheres are not robust, homogeneous and stable systems for propagation of large number of cells *in vitro* [18].

As an alternative to neurospheres, adherent cultures support the propagation of NSCs in an easier way to control. The work of Conti et al. [19] and Pollard et al. [20] demonstrated the importance of the combination of EFG and FGF to suppress differentiation in long- term adherent cultures. They found that, with the provision of both factors, the populations generated were more homogeneous, had a higher neurogenic potential compared to neurospheres, maintained multipotency for several passages and expanded symmetrically. Furthermore, cells in this system are uniformly exposed to the growth factors and are easily monitored [9]. Pollard *et al* [20] also addressed the issue of detachment and cell aggregation at higher densities and at earlier passages by coating the plates with gelatin or poly-ornithine/laminin. Several reports of successful *in vitro* long term expansion of different NSCs as monolayers have been described, including the cells used in this work, lt-NES [16, 17]. Moreover, other strategies for adherent cell culture are being evaluated namely, using microcarriers and encapsulation in matrices [21].

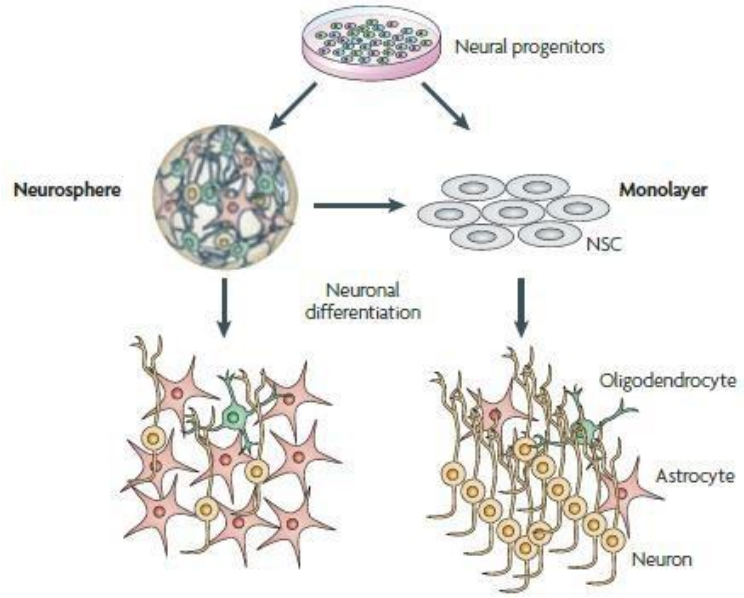

Figure 3: NSCs *in vitro* culture systems and outcomes of neuronal differentiation. Adapted from [7].

1.1.3.4 Applications of NSCs

The ability of stem cells to produce new cells in response to injury or disease as well as their protective role predicts their therapeutic benefits if mobilized to such affected regions. Transplantation can thus be the answer in brain regeneration to the low numbers of adult NSCs in the brain and the proliferation decline with aging. NSCs survival and functional benefit has been documented in several regions of the CNS of rodents and nonhuman primates following transplantation [22-25]. However, some other questions arise when translating NSC research to clinical practice, such as their ability to migrate to the correct injured site, to integrate into the host tissue and to survive in the host environment [26]. Furthermore, safe strategies to produce enough numbers of cells for therapeutic and research applications are needed as well as robust protocols to generate highly pure cell lines. Some clinical trials are already being conducted to assess the therapeutic value of such transplants: fetal-derived human NSCs are being tested in patients with spinal cord injury and retinal disease dry age-related macular degeneration (AMD) [27].

The understanding of the human CNS development has also been improved in the last years due to the resemblance of *in vitro* neural differentiation steps to embryonic neurogenesis. The recent description of the formation of a three-dimensional (3D) brain tissue, called cerebral organoids, is an exciting example of an in *vitro* culture capable of recapitulating various human brain regions and similar organization to the developing brain [28].

Furthermore, the roots of human neurological diseases are a permanent research question for neuroscientists scientific community, to which reprogramming technology have shed some light on. It is now possible to establish relevant disease models from iPSC-derived neural cells to study pathological mechanisms that lead to neurodegeneration. Parkinson´s disease, Alzheimer´s disease, Rett syndrome, multiple sclerosis and amyotrophic lateral sclerosis are some of the diseases whose phenotype has been modeled *in vitro* from differentiated human iPSCs derived directly from patients [29, 30]. These disease representations are useful as well to generate drug screening platforms to predict the efficacy of novel drugs, circumventing the inaccuracy of animal models, the limited information on how a patient may respond to a particular drug, thus avoiding failures of clinical trials.

1.2 Scale-Up Culture Strategies

Conventionally, the standard approach for stem cell culture has been based on static two-dimensional (2D) surfaces, like plastic plates or tissue flasks due to their simplicity, easy handling and low cost [31]. For instance, adherent cells have been grown as monolayers on protein treated or uncoated plastic dishes or on top of feeder cells (e.g. mouse embryonic fibroblasts). However, such systems fail to mimic 3D *in vivo* conditions, regarding cell-cell and cell- extracellular matrix (ECM) interactions and integration of biophysical signals (mechanical, electrical, hydrodynamic) [32].

Moreover, scale-up of cell culture using 2D planar platforms for applications such as cell replacement therapy or drug screening tests is hardly feasible. Their low productivity due to the limited surface area available for cell growth requires the maintenance of multiple culture vessels simultaneously in order to produce relevant cell numbers. That implicates frequent cell passaging since vessels are restricted to one log of expansion, leading to extensive manual handling; will require laborious feeding procedures that may increase contamination risks as the number of units to handle increase. Also, such platforms are difficult to be monitored and controlled, leading to variation between units within a batch, affecting the accuracy of the results [33].

To exploit the clinical and industrial potential of stem cells and their derivatives, scale-up will require automated, more productive systems which must be reproducible, robust and cost-effective [33]. Such systems must address some key challenges to resemble tissue dynamics: they will have to provide adequate, uniformly distributed influxes of oxygen and nutrients at physiological concentrations, removal of carbon dioxide and metabolites and accommodate support materials for adherent cells. Moreover, cell harvesting procedures must also be addressed to ensure cell integrity.

1.2.1 Bioreactor systems for stem cell culture

In general, systems operating at dynamic conditions satisfy the criteria mentioned above. There are several configurations of bioreactors which provide dynamic cultures: roller bottles, spinner flask, stirred

bioreactor, air-lift bioreactor, hollow fiber, fixed or fluidized-bed bioreactor, wave bioreactors and rotary cell culture systems, which will be briefly described in this section.

Roller bottle culture (*Figure 4a*) is based on multiple cylindrical bottles placed in a rotating device, where cells are alternatively exposed to medium and the gas phase, allowing a more efficient oxygenation. The entire internal surface of the bottles is available for cell growth, allowing higher unit cell densities. This modality can accommodate up to hundreds of bottles but that also implies an increase in costs and handling.

The stirred suspension bioreactors, including spinner flasks and stirred-tank bioreactors (*Figure 4b*), are relatively simple systems that use mechanical stirring to provide a homogeneous environment. High cell concentrations can be obtained in a controlled mode of operation, where it is possible to monitor biochemical and physical parameters (e.g., oxygen tension, pH, medium exchange rates, glucose concentration), which are very important when the final application is a therapeutic product. Different types of impellers (e.g. marine blade, cell lift) may be used to promote different agitation schemes and minimize the force exerted over the cells due to the flow of the media, named shear stress [31, 34]. Stirred suspension bioreactors can be combined with different 3D cell cultures (microcarriers, encapsulated cells, cell aggregates) to increase productivity, and stirred tank bioreactors, in particular, provide mass transport through different modes of operation (batch, fed-batch, perfusion) [33]. Perfusion is particularly advantageous, since fresh medium is continuously added and older medium removed while the cells are retained within the reactor. This mode is preferable when cell products are toxic or there is the need to use small volumes. Scale-up with stirred tank bioreactors is usually preceded by spinner flasks (*Figure 4c*), which are small vessels, whose size ranges from a few milliliters to 20L, with an agitator to provide a mixed environment for cell culture in suspension.

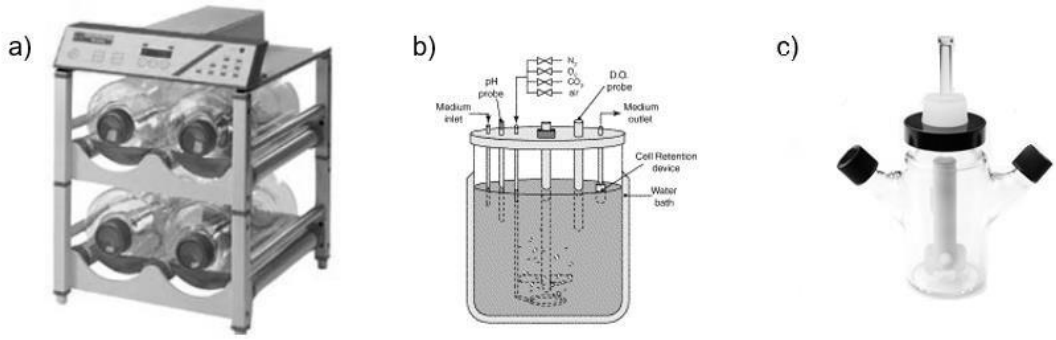

Figure 4: Several bioreactor configurations. a) Roller botlles; b) Stirred tank; c) Spinner flasks (Adapted from [35-37])

Stirring is not only promoted by using mechanical devices, air-lift bioreactors use air or oxygen bubbled into the bottom to stimulate circulation. In this case, the height-diameter ratio must be high to improve motion and minimize cell damage (*Figure 5 a*).

Wave bioreactors eliminated the need for sterilization and cleaning by using a disposable, sterile bag which is placed in a rocking platform, allowing to work under good manufacturing practices (GMP). The bag is partially filled with media and oxygen transfer occurs due to the motion waves induced in the media by the platform (*Figure 5 b*). Despite these wave reactors have the requirements to generate products suitable for clinical application, their high costs may hinder its use.

The basis of the hollow fiber bioreactor is the growth of cells in the extra capillary space that surrounds semi-permeable fibers. The medium is carried by the capillaries, nutrients and gases diffuse through the hollow fiber membrane and pH and oxygen saturation are adjusted after each passage. Ceramic matrix module is a variation of the hollow fiber bioreactor, with the exception that cells are not separated from the medium flow by a membrane (*Figure 5* c).

Adherent and non-adherent cells can be cultured in packed bed bioreactors, where they are immobilized in a stationary matrix (e.g. micro spheres or fibers, macrocarriers for non-adherent cells) placed in a column (the bed) composed of packed particles (*Figure 5 d*). The bed is perfused with culture medium and the reactor can operate under batch, fed-batch or continuous perfusion modes, with possible control of culture parameters. Concentration gradients of nutrients and waste products may occur and sampling of cells is not possible. Fluidized bed bioreactors differ in the floating particles that constitute the bed and may cause shear stress [38].

Lastly, rotating wall vessels are composed by a rotating cylindrical vessel that simulates microgravity conditions, have low shear stress and provides a mixed environment and efficient gas transfer, but scale-up of this bioreactor configuration to large volumes is not straightforward (*Figure 5 e*) [33].

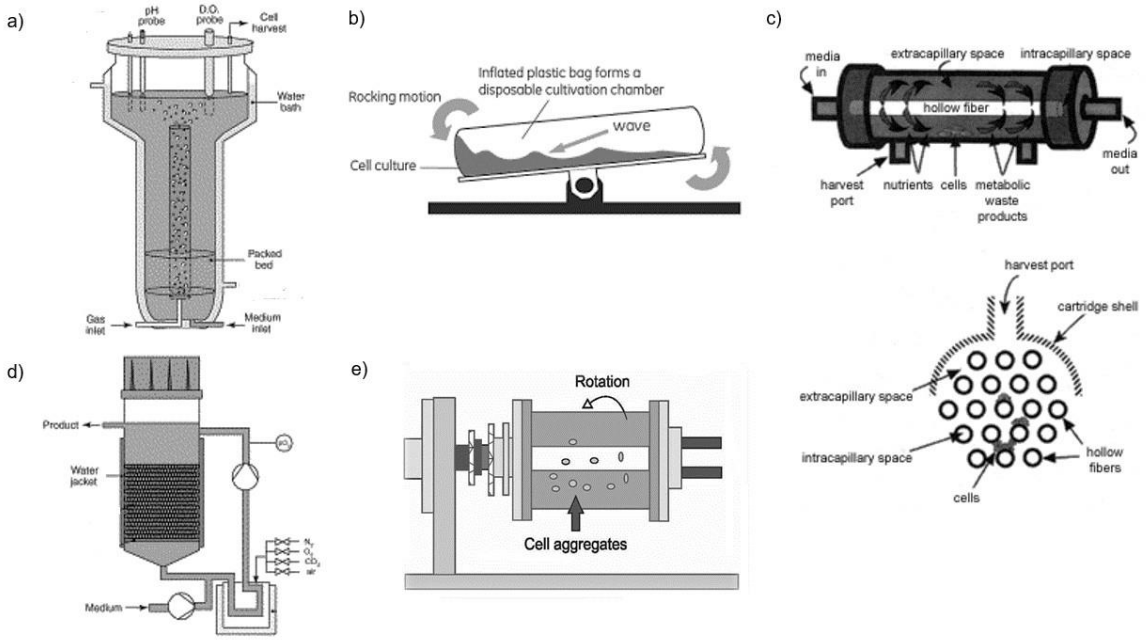

Figure 5: Several bioreactor configurations. a) Air lift ; b) Wave bioreactor; c) Hollow-fiber; d) Fixed or fluidized bed; e) Rotating-wall vessel. Adapted from [36, 39-41]

Despite the various existing devices, there is not an optimal and universal system for scale-up. There is still room for design improvements and optimization of culture conditions depending on the specific cell type. Hydrodynamic shear stress, for example, must be addressed through the design of different impeller configurations and variation of agitation speeds. The lack of cell wall in animal cells makes them sensitive to the forces created by the agitation, therefore, rates of flow media may exert various effects on cell expansion and differentiation. High flow rates can be responsible for cell disruption or slow growth, and, on the other hand, low flow rates could lead to cell clumping or aggregation [34]. Extensive research to determine the optimal values for critical parameters like dissolved oxygen, pH, perfusion rates, concentration of nutrients, growth factors, cytokine and many others is also necessary [42, 43].

Computer-controlled bioreactors to monitor and control those variables pave the way towards more automated platforms in real time and will be key players in the efficient production of high quality products for clinical applications. Mathematical models will also be valuable to predict stem cell behavior, process outcomes and aid in the optimization of the culture conditions at lower costs.

1.2.2 3D culture systems

The capacity of stirred-tank bioreactors to support 3D culture strategies allowed the transition of anchorage-dependent cells from small to large-scale production. Developments in the field of biomaterials contributed significantly to create support materials to substitute tissue culture plates, in which adherent

cells could grow while taking advantage of the stirred vessel setting. Moreover, the influence of the native ECM geometry in cell function and identity is recapitulated more closely in the microenvironments provided by the 3D systems. Therefore, this approach may result in more accurate extrapolations to what is really occurring *in vivo* [33].

Various 3D suspension culture systems have been developed to promote the expansion of stem cells, such as cell encapsulation in biomaterials, cell aggregates, cells immobilized on microcarriers, and other 3D scaffolds (*Figure 6*). Microcarriers will be detailed in section 1.4.

.

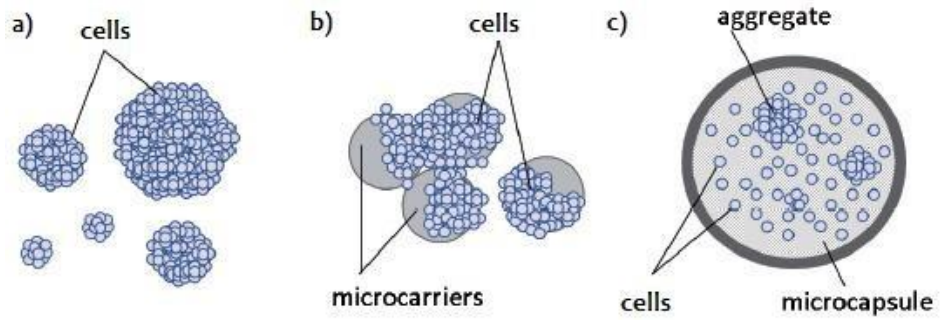

Figure 6: Representation of 3D culture systems. a) cell aggregates; b) Microcarriers; c) Encapsulated cells; Adapted from [33].

1.2.2.1 Cell aggregates

Culturing cells as self-aggregated spheroids allows the simulation of the native microenvironment, since cells maintain 3D contact between them. However, they are heterogeneous cultures since cells at the surface and core of the aggregate are differently exposed to culture media, oxygen and metabolic products, which could result in the formation of necrotic zones at the core. To prevent those, aggregate size can be controlled by means of agitation in stirred bioreactors [33]. 3D aggregates are used for the differentiation of ESCs, through the formation of EB, and for NSC cultivation and differentiation as neurospheres, which were already discussed.

1.2.2.2 Cell encapsulation

In encapsulation, cells are immobilized within a semipermeable microcapsule that allows diffusion of mass and gas. This represents an alternative to aggregates and microcarriers since it prevents excessive cell agglomeration, protects cells from shear stress and preserves 3D native configurations. Alginate is a common material used for encapsulation, in combination with polylysine (pLL) [44]. A great advantage is the possibility to customize different biomaterials according to the application, aiming to improve culture

outcomes. Far from being an ideal system, encapsulation has several disadvantages such as the limitations in oxygen and nutrients diffusion inside the capsule, cell harvesting and difficulty in culture visualization and monitoring [33]. Cell encapsulation as a tool for transplantation may avoid immunorejection, thus, reducing the need for long-term immunosuppression, and it may allow the controlled delivery of therapeutic molecules, improve cell survival and engraftment *in vivo*.

1.3 Microcarriers

In 1967, Van Wezel described microcarriers for the growth of anchorage-dependent cells. By that time, those particles were used in other biological applications, including viral vaccines and antibodies production from mammalian adherent cells [45]. Currently, with the improvement of bioreactors compatible with microcarriers (stirred, wave, packed and fluidized-bed bioreactors), they have become a successful scale-up method for high density perfused cultures.

Microcarriers are small spheres that allow the immobilization of adherent cells while in suspension in stirred cultures. Cells are mixed with the beads, attach to their surface, spread and grow as monolayers until contact confluence.

1.3.1 Microcarriers properties

A variety of microcarriers are now commercially available, composed of different materials and having different shapes, sizes, porosity and surface modifications (*Table 1*). Despite this, there is still scope for design of cell-compatible microcarriers to optimize specific cell cultures since it has been shown that microcarrier properties affect differently cell attachment, growth rates and potency [38].

Microcarriers diameter vary from 100 to 400µm and size distribution should be as narrow as possible in order to prevent heterogeneous distribution of cells [46]. They can be made of inorganic materials, such as glass, silica and ceramics, or of organic natural polymers (e.g. collagen, alginate, gelatin…) or organic synthetic polymers (such as polystyrene, polyacrylamide, polyester, polyethylene, etc.). They can contain surface modifications to include functional groups or proteins for example, -COOH or -NH_2 polystyrene resins used in this work or gelatin-coated dextran beads (Cytodex 3). Density of microcarriers is also variable, normally being slightly higher that the density of cell culture medium/water to allow microcarrier suspension [46]. Ideally, the particles should be transparent for direct observation of the cells, withstand sterilization and be mechanically stable throughout cultivation [47].

Table 1: Characteristics of some commercially available microcarriers.

Commercial name	Manufacturer	Core material	Surface chemistry/coating (charge)	Diameter (μm)	Surface Area (cm^2/g)
Cytodex 1	GE Healthcare	Crosslinked dextran	Tertiary amine throughout the matrix (+)	147-248	4400
Cytodex 3	GE Healthcare	Crosslinked dextran	Denatured collagen (none)	141-211	2700
Plastic	Pall Life Sciences	Crosslinked polystyrene	None	125-212	360
Plastic Plus	Pall Life Sciences	Crosslinked polystyrene	Cationic (+)	125-212	360
Pronectin F	Pall Life Sciences	Crosslinked polystyrene	Recombinant protein (+)	125-212	360
Cultispher S	Percell Biolitica	Gelatin	None	130-380	-
Hillex II	Pall Life Sciences	Modified polystyrene	Cationic trimethyl amine (+)	160-200	515
Glass	Sigma	Crosslinked polystyrene	Silica glass (none)	125-212	360
Collagen	Pall Life Sciences	Crosslinked polystyrene	Gelatin (none)	125-212	360

Microcarriers can be classified regarding their porosity in microporous or macroporous. In macroporous beads, such as Cultispher S, cells are able to grow inside the pores, which reduces their exposure to mechanical (stirring) and chemical stress (lactate and ammonia) at the surface. On the other hand, if the beads are not degradable, removing cells from the pores can be a difficult task, in such cases, it may be preferable to use solid microcarriers. In addition, cells inside the pores are exposed to a different environment, with limited access to nutrients [48].

This technology is more advantageous than 2D planar systems since it provides a higher surface-volume ratio: one gram of plastic microcarriers (manufactured by Pall/SoloHill) has a surface area equivalent to five 75cm^2 culture flasks. Therefore, it allows higher cell densities per volume and the available surface area can easily be adjusted by changing the amount of microcarriers. Compared with 2D platforms, microcarrier systems reduce costs with medium and growth factors, and saves incubator space. Compared to cell culture as aggregates, the environment of the culture with microcarriers is more homogeneous, since cells grow as monolayers, being equally exposed to nutrients and growth factors. A challenge regarding this system is the efficient cell harvesting from the beads without loss of cell integrity. Gelatin or collagen microcarriers can be a solution, since they are susceptible to enzymatic degradation [49]. In addition, cell separation from the microcarriers has to be guaranteed when the final goal is a

therapeutic application, which may be aided by the use of magnetic beads [50]. Microcarrier concentration must also be optimized since higher concentrations can result in bead-to-bead or bead-to-cell collisions and microcarrier suspension may become difficult to manipulate. Moreover, commercially available microcarriers are not optimized for the long term propagation of stem cells and additional ECM coatings are often required to improve culture performance [48].

1.3.2 Adhesion to microcarriers

Cell attachment to a substratum is mediated by nonspecific physical forces and specific adhesion interactions promoted by certain molecules. Among nonspecific physical forces are the electrostatic forces, that occur between charged particles, and van der Waals forces, that arise between electrically neutral particles [51]. Electrostatic forces are repulsive if the bodies are of the same charge and attractive when of opposite charge. Stem cells have negatively charged surfaces and can be cultured on positively charged substrates, such as diethylaminoethyl **(**DEAE)-dextran, or pLL, being repelled, in theory, from materials such as plastic and glass that have negative charge. However, it appears that charge density plays a more critical role than the polarity of charge in cell attachment since cells can adhere to both negative and positive surfaces [49].

After the first nonspecific interactions, attachment and spreading of the cells rely on the specific adhesion interactions. Those are mediated by cell-adhesion molecules, which can be secreted by some cells or are naturally present in media supplemented with serum, and are adsorbed by surfaces, allowing cells to directly adhere to them. In serum-free conditions however, attachment proteins or peptides must be dissolved in the medium or coated into the surfaces. Collagen, laminin, vitronectin, fibronectin, proteoglycans, the ligand arginine-gycine-aspartic acid (RGD) sequence, which is the cell recognition site for a number of ECM proteins, are examples of ECM molecules involved in the adsorption process. The final step is the spreading of the cells onto the surface which is possible due to cytoskeletal rearrangement without whom cells would not proliferate. [51].

Summing up, an ideal surface for cell attachment would combine electrostatic charge and adhesion promoting molecules. Electrostatic charge is responsible for rapid cell attachment while ECM protein coated surfaces allows cell spreading and growth.

1.3.3 Materials and surface properties

Cells have been cultured in microcarriers made of numerous materials, whether they are natural or synthetic polymers or even inorganic materials. Since all of them have different properties, such as optical, physico-chemical and mechanical properties, they will have distinct interactions with the cells and will affect their behavior, thus, it is fundamental to use appropriate materials for each cell type.

Natural materials are usually biocompatible but face several limitations such as the animal source and its availability, the requirement for complex processes to isolate and purify the materials and batch-to-batch variations [52]. It is difficult to tune the mechanical properties and crosslinking is generally necessary to enhance stability. Alginate, collagen, cellulose and gelatin are natural polymers that have been used in cell culture since they integrate native biochemical signals [52]. On the other hand, synthetic materials are scalable, reproducible, have low immunogenicity and have more controlled properties regarding their structure, molecular weight, hydrophobicity, mechanics, therefore, are easily reproduced. Nevertheless, they do not mimic living tissue matrices and lack specific cellular stimulation which can be ameliorated with bio-functionalization [52].

The characteristics of the surface material also play a fundamental role since the interaction between cells and substrates occur at the surface. Charge density, surface topography, hydrophobicity (wettability), mechanical stiffness, chemical composition and surface modifications are some of the factors that may determine efficiency of cell adhesion and enhance growth if they provide cues that closely resemble the *in vivo* environment [46]. As mentioned, charge density has been pointed out as more relevant than charge polarity: cell attachment and growth would certainly benefit from the establishment of an optimal value. In fact, if charge density is low, cells will detach easily, on the other hand, if it is high, cells will adhere rapidly but wo not spread and grow, and on top of that, are more difficult to separate from the particles [47]. Rigidity also influences stem cell fate. It was recently shown that rigid substrates support maintenance of pluripotency of hESCs, while softer ones led to differentiation, which indicates hESCs are sensitive to the mechanical environment [53].

1.3.4 Surface Functionalization

In order to increase the efficiency of cell attachment in synthetic materials or that lack cell recognition sites, several strategies to modify surfaces of scaffolds have been considered: charging the surface, improving its hydrophilicity, coating with adhesion-molecules. Copolymerization with ionic monomers, low temperature plasma are techniques that provide electrical charge [47]. Hydrophobic surfaces can be subjected to alkaline hydrolysis, laser or plasma treatment to improve hydrophilicity [54].

Coatings in 2D substrates with ECM proteins are commonly performed by physical adsorption, which can also be translated to 3D systems. When such molecules are coupled to the surfaces, attachment and spreading are improved. Microcarriers coated with Matrigel, collagen, laminin and other molecules have been successful in the culture of human PSCs [48, 55, 56]. Particularly, Chen *et al* [48] investigated the effect of uncoated and laminin or Matrigel coated beads in static conditions. Despite the high attachment efficiency observed in uncoated microcarriers, lower cell yields were obtained and a tendency to differentiation was exhibited, as opposed to Matrigel or laminin coated beads, which supported long term propagation of hESCs. Physical adsorption, however, may not provide a strong stability to the cell adhesive proteins due to the weak interactive forces, which may be surpassed by covalent links [54].

Techniques to covalently conjugate molecules to a specific substrate include carbodiimide-mediated coupling, glutaraldehyde crosslinking, ultra-violet (UV) light, aminolysis, among others [57-60]. As an example, growth factors were covalently immobilized on microcarriers either by the carbodiimide EDC and NHS reaction or riboflavin/UV light-mediated crosslinking in order to enhance cell attachment [57]. The rationale behind this work was to prevent early burst release of the growth factors with surface immobilization through covalent bounds introduced by crosslinking. Carbodiimide conjugation was also performed in the work of Fan *et al.* [58] in which RGD-containing vitronectin was conjugated to polystyrene beads with –COOH groups on their surface via EDC/NHS reaction. Cells proliferated in peptide-conjugated microcarriers in static cultures but when under stirring in spinner flasks, extensive aggregation occurred and cells detached from the beads. To further strengthen the link between the cells and the surface, microcarriers were additionally treated with pLL, a positively charged synthetic polymer which enhanced cell attachment.

In the present work, the microcarrier surface was functionalized with laminin which was conjugated either through physical adsorption or carbodiimide based reaction when in the presence of functional groups. This technique will be characterized next.

1.3.4.1 EDC/sulfo-NHS coupling

EDC/sulfo-NHS reaction is a coupling chemical reaction which conjugates proteins with other proteins, peptides, nucleotides or particles. EDC (1-ethyl-3-(3-dimethylaminopropyl) carbodiimide) is a water-soluble, biocompatible carbodiimide used to conjugate carboxylates (–COOH) to primary amines ($–NH_2$) through the catalysis of an amide bond [61]. -NHS or sulfo-NHS (N-hydroxy sulfosuccinimide) are hydrophilic groups used to increase the stability of the intermediate formed in the reaction between EDC and carboxyl groups, via the formation of an active ester functional groups with carboxylates [61]. EDC-sulfo NHS reaction occurs in two steps: activation and coupling. First, free carboxyl groups react with EDC and form active esters in the presence of NHS or sulfo-NHS. This first activation phase can be terminated by adding β-mercaptoethanol which deactivates EDC, thus, blocking activation of remaining carboxyl groups. From this point, a second protein or particle containing amine groups can be added and amide crosslink occurs between the two compounds (*Figure 7*) [62].

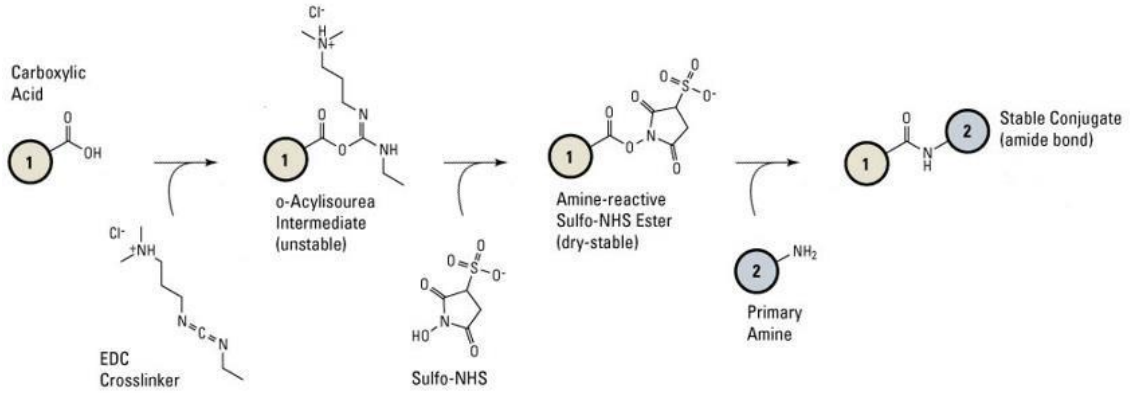

Figure 7: EDC/sulfo-NHS coupling reaction scheme. (1) and (2) can be proteins, peptides or chemicals containing carboxyl or primary amine groups, respectively [63].

This crosslinking method is one of the most important to covalently attach peptides or other molecules to a surface material, and is commonly used for peptide immobilization for affinity purification, to label carboxyl groups with amine compounds or to conjugate peptides to carrier proteins [63].

1.3.4.2 Coating substrates and molecules

The biological molecules usually applied in coating procedures are the components of basement membranes, which are extracellular structures containing glycoproteins. Matrigel is one of the first cell adhesion coatings described for the propagation of human PSCs under feeder-free conditions and is still commonly used. It is a basement membrane preparation derived from mouse sarcomas, composed of many components, including laminin, collagen IV, entactin, proteoglycans and growth factors [64]. One of its components and the main one of basement membranes, laminin, is also applied individually as a coating substrate in cell culture, including NSCs culture. Laminin is a high molecular weight protein composed of three polypeptide chains joined together with disulfide bonds that it result in a “T”-shaped structure (*Figure 8*). It is responsible for several biological activities, including stimulation of growth and differentiation, neurite outgrowth promotion, promotion of cell attachment, mediation of cell communication and interactions between basement membrane components [65]. Other proteins extracted from animal sources that also possess cell recognition and adhesion motifs are collagen, fibronectin, vitronectin and gelatin.

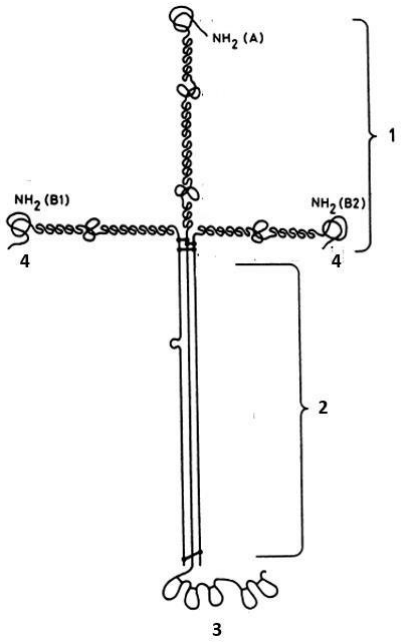

Figure 8: Laminin structure. Chains A, B1 and B2 each containing the NH_2 terminus. 1) ECM assembly; 2) triple coiled-coil represented by parallel straight lines; 3) cell-surface receptor binding domain; 4) collagen binding domain. Adapted from [65].

Such biological molecules are difficult to exploit given their large molecular weights (e.g. laminin is 850 000 Da), their complex and costly isolation and purification processes, subject to batch-to-batch variations. It also may be difficult to obtain them from large-scale and high-quality sources [52]. Laminin is an example of a protein difficult or impossible to isolate in native form from tissues, only recently being produced as a recombinant protein. Hence, development of cost-effective bioactive synthetic coatings, fully defined, safe, xenogeneic-free and capable of supporting proliferation and potency, represent significant milestones [66].

Among the synthetic coatings develop thus far are the examples of the polymers poly[2-(methacryloyloxy)ethyl dimethyl-(3-sulfopropyl)ammonium hydroxide] (PMEDSAH) and aminopropylmethacrylamide (APMAAm), which sustain long-term expansion of hPSCs or Synthemax, which is constituted by an acrylate polymer functionalized with short amino-containing peptide sequences derived from vitronectin [64]. Polycations such as pLL or poly-ornithine, which are synthetic amino acid chains, are also used as coatings either alone or in combination with other molecules.

1.4 Scale-up strategies for NSC

Extensive work has been done to develop and optimize technologies to expand NSCs in high quantities, overcoming the limitations of standard static conditions and the weaknesses of neurospheres. Culture of mouse NSCs as aggregates in stirred reactors have been successfully described, particularly by the group

of Behie [67, 68]. The author have addressed critical parameters to optimize scale-up mouse NSC protocols, regarding inoculation strategy, oxygen transfer, growth conditions, among others. Adequate agitation rate was found sufficient to control aggregate size, preventing excessive agglomeration and allowing a more uniform distribution of mass and gases. Based on these works, Gilbertson *et al* [69] reported the expansion of mouse NSCs in 500 mL suspension bioreactors under computer-controlled conditions. The process enabled the generation of a maximum cell density of 1.2×10^6 cells/mL without affecting multilineage potential.

Besides the expansion as neurospheres, other 3D platforms have also been combined with bioreactors. Mouse-derived NSCs were expanded in microcarrier suspension stirred bioreactors in a study conducted by Rodrigues *et al.* [43]. Different commercially available microcarriers were tested in static cultures and the best results were achieved with Pronectin F microcarriers, which are polystyrene spheres with surface charge coated with a protein-polymer engineered to promote cell adhesion. This system was then transferred to a spinner flask and further optimized regarding medium change rates, stirring scheme and agitation speed, which resulted in an almost 35 fold increase in cell number without loss of viability, multipotency and maintenance of NSC markers such as Nestin and Sox2. Another work showed the feasibility of the immobilization of rat NSCs cells in collagen gels and its propagation in rotary wall vessels. Data indicated the long-term proliferation and differentiation capacity of cells entrapped in a 3D matrix, which formed aggregates without the formation of necrotic centers. Notably, it was documented a 10-fold increase in the generation of Nestin and GFAP positive cells and a greater expression of Tuj1 (neuronal marker) [70].

Despite the important results obtained so far with mouse NSCs, those have to be translated to human cells given the behavior differences between the two cell line species [68]. Having this in mind, Rodrigues *et al*. described the expansion of human lt-NES in Pronectin-F spinner flask bioreactors, adherent to microcarriers, with a maximum of 3.5 fold increase in cell number [71]. Significant quantities of human neural progenitor cells were also generated by different authors, safely, using the PPRF-h2 serum-free medium in suspension bioreactors. Those bioreactor expanded cells were already successfully transplanted into a rat model of Parkinson´s disease [72].

Expansion of NSCs, particularly using microcarriers, in suspension bioreactors has tremendous potential, but optimization of protocols is still a major requirement; it needs to be taken into account the characteristics of each cell type when choosing the suitable microcarrier for culture. Inoculation strategy (initial cell density, single cells vs clumps), stirring mode (intermittent vs continuous), feeding scheme, agitation speed will also affect in different ways the expansion of cells in a given material. Agitation rate, for example, influences the initial distribution of cells in microcarriers and prevents excessive aggregation of the particles [43]. An important parameter to be considered also is the microcarrier concentration, given that the available surface area will affect cell growth.

1.5 Aim and Motivation of Studies

Nowadays, importance of stem cells is widely recognized both in the scientific research field and in clinical practice. Given their unique features, scientists envisioned stem cell as potential medical therapies, for example, to replace damaged cells or regenerate tissues or organs. Neural stem cells (NSCs), in particular, are expected to be used in the future in the treatment of major neurodegenerative disorders, including Parkinson's and Alzheimer's diseases.

In order to match that expectation, large-scale technologies are required to support expansion of relevant cell numbers without compromising their functional properties. NSCs can be cultured as anchorage-dependent cells, using planar surfaces like tissue culture plates or flasks. Those, however, are not suitable to generate the quantities intended for therapies. Microcarriers provide a surface for cell adhesion while maintained in suspension. Combining microcarriers with bioreactors allows the development of scalable systems, highly controlled regarding critical culture parameters, including shear stress, temperature, pH, diffusion of nutrients, oxygen and metabolic products. There are several microcarriers commercially available but there is a great need to design microcarriers tailored for the expansion of specific stem cell lines.

Surface properties of the microcarriers, or of any scaffold, are known to influence cell growth and fate, which explains much of the work described in the literature regarding microcarrier functionalization in an attempt to mimic the *in vivo* stem cell microenvironment. Usually, surfaces for cell adhesion are coated with ECM proteins through physical adsorption which does not provide strong interactive forces between the cells and the substrate. It was hypothesized that such forces would not be stable in stirring conditions, resulting in the release of the ECM molecules and subsequently, the cells from the microcarriers. Therefore, it was proposed that surface conjugation of microcarriers based on a covalent bond with ECM proteins would improve the stability of the protein coating and likewise the efficiency of cell attachment and proliferation.

This project aimed the development of improved microcarriers for NSC culture. Selected microcarrier particles were thus functionalized by surface conjugation using two different techniques and a comparison of their performance for NSC culture under static and dynamic conditions was performed. To accomplish this goal, this work was conducted according to the following main tasks:

- Conjugation of laminin to microcarriers through the EDC/sulfo-NHS crosslinking reaction and quantification of the protein attachment efficiency.
- Screening of different types of microcarriers, with different coatings, for lt-NES cell culture under static conditions.
- Optimization of the laminin concentration required for adsorption or EDC/sulfo-NHS crosslinking to microcarriers to be used for lt-NES cell culture.

- Comparison of lt-NES culture under dynamic conditions using microcarriers functionalized through adsorption or EDC/sulfo-NHS crosslinking.

1.6 Novelty

This work addressed the comparison of two coating procedures, adsorption and crosslinking, in protein immobilization to commercially available microcarriers and in cell culture under static and dynamic conditions. It was already reported in the literature the functionalization of microcarriers with a protein fragment through crosslinking, whereas, this project aimed at the functionalization of microcarriers through crosslinking with a whole protein, in this case, laminin. The functionalized microcarriers were cultured with a specific type of neural stem cells, lt-NES, which were used given their capacity to self-renew for more than 100 passages while maintaining the neuronal differentiation.

2 Materials and Methods

2.1 Microcarriers preparation and bio-functionalization

Different commercially-available animal-free microcarriers were tested under static conditions with different coatings. The microcarriers were: Polystyrene AM NH_2, Carboxy Polystyrene (both from RAPP Polymere), Cytodex 1, Cytodex 3 (both from GE Healthcare) and Plastic (Pall Life Sciences) (*Table 2*). Polystyrene AM NH_2 and Carboxy Polystyrene beads present a capacity of 1.11mmol/g of $–NH_2$ and of 2.01mmol/g of –COOH groups on their surface, respectively, allowing for protein conjugation via an EDC/NHS reaction.

Table 2: Properties of the microcarriers used in this work. Note: * cm^2/ dry weight.

Product	**Material**	**Average Diameter** (µm)	**Area** (cm^2/g)	**Density** (**g/cm^3**)
Plastic	Crosslinked polystyrene with no surface charge	169	360	1.022-1.03
Cytodex 1	Cross-linked dextran matrix substituted with positively charged N, N-diethylaminoethyl groups	190	4400*	1.03
Cytodex 3	Crosslinked dextran coupled with a thin layer of collagen	175	2700*	1.04
Carboxy Polystyrene	Polystyrene resin featuring -COOH groups on the surface	180	356.3	1.03
Polystyrene AM NH_2	Polystyrene featuring $–NH_2$ groups on the surface	180	356.3	1.03

Cytodex 1 and Cytodex 3 were prepared prior to use according to manufacturer´s recommendations: microcarriers were swollen and hydrated in phosphate buffered saline (PBS, Gibco) using 50-100mL/g Cytodex 1 or 3, for at least 3h at room temperature. The supernatant was removed and the microcarriers were washed in PBS (30–50 ml/g Cytodex 1 or 3). All of the microcarriers were sterilized with ethanol 70% for 1h at room temperature, using a rocking platform mixer, washed twice with sterile PBS and kept in 15mL Falcon tubes (Corning) with sterile PBS, at room temperature until functionalization and/or cell culture.

The microcarriers were coated using two strategies: via a covalent bond through EDC/sulfo-NHS reaction, or through adsorption of poly-ornithine and mouse laminin (both from Sigma) to the beads. Unless mentioned otherwise, laminin was crosslinked at a concentration of 14µg/cm^2 and adsorbed at 3µg/cm^2.

2.1.1 Surface functionalization via EDC/NHS crosslinking

Microcarriers with functional groups on the surface were coated with laminin through EDC/sulfo-NHS crosslinking. This reaction occurs in two steps: the activation of the -COOH groups of the first protein/particle and then, coupling to amine groups of the second protein/particle (*Figure 9*). The two types of beads (-NH_2 and -COOH) were conjugated via EDC/NHS reaction following slightly different protocols adapted from Thermo Scientific [73] given the different functional groups: -COOH beads required the activation step and the amine containing beads were introduced in the coupling step.

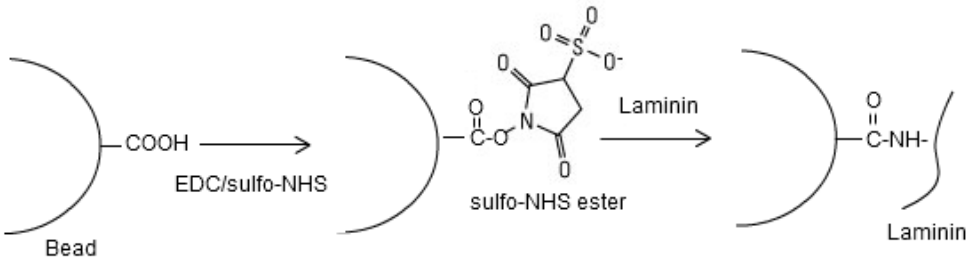

Figure 9: Schematics of EDC/sulfo-NHS mediated covalent attachment of laminin on the surface of carboxyl polystyrene beads.

Carboxyl microcarriers were submitted to the following protocol: 30mg of beads (≈11cm^2) were prepared in 3mL activation buffer (0.1M MES (2-[morpholino]ethanesulfonic acid, Sigma)), 0.5 M NaCl at pH 6.0. Sulfo-NHS (N-hydroxy-Sulfosuccinimide, Acros Organics) and EDC (1-ethyl-3-[3-dimethylaminopropyl]carbodiimide, Sigma) were added to the microcarriers at a final concentration of 5mM and 2mM, respectively, to activate the carboxyl groups, and mixed for 30mins at room temperature. Then, excess liquid was removed and beads were washed twice with PBS and incubated overnight with the laminin (Sigma**)** solution in PBS in the desired concentration, at pH 7.2-7.5, with magnetic stirring. After overnight incubation, beads were washed twice with PBS, incubated in a 100mg/mL glycine (Sigma) solution for 1hour to quench the reaction, at room temperature with agitation, and washed once with PBS.

Amine containing beads were submitted to the following protocol: laminin solution in PBS in the desired concentration was dissolved in 3mL activation buffer. Sulfo-NHS (N-hydroxysuccinimide, Acros Organics) and EDC (1-ethyl-3-[3-dimethylaminopropyl]carbodiimide, Sigma) were added to the solution prepared previously at a final concentration of 5mM and 2mM, respectively, and mixed for 30mins at room temperature. To quench the reaction, 20mM of 2-mercaptoethanol (Sigma) was added for 10min. The pH

of the solution was increased to pH 7.2-7.5 by adding drops of 1M NaOH and 1mL of 10X PBS was added to buffer the solution. 30mg of amine containing beads (≈11cm^2) were added to the mixture solution and left overnight at room temperature with magnetic agitation. Then, beads were washed twice with PBS, incubated in a 100mg/mL glycine solution for 1hour, at room temperature with agitation, and washed once with PBS.

2.1.2 Surface functionalization through adsorption

A poly-ornithine/laminin coating was performed on Plastic microcarriers, Cytodex 1 and Cytodex 3. As controls untreated microcarriers of each type and poly-ornithine coated Plastic microcarriers were used as well. PBS was removed from the tubes with microcarriers and poly-ornithine was added for 1 hour in a rocking platform mixer. Beads were washed with sterile PBS and incubated with a 25µg/mL laminin solution in PBS for 3 hours with agitation. After that period, solution was removed and microcarriers were washed and maintained in culture media until cell seeding.

2.2 Crosslinking reaction validation using the Bradford assay

The Bradford assay is a protein quantitation method based on the binding of the Coomassie dye to the protein, which causes a shift in the absorption maximum of the dye from 465 to 595nm, with a color change from brown to blue [74]. This method was employed to validate the EDC/sulfo-NHS crosslinking reaction between the laminin and the -COOH beads.

Samples of the supernatant from microcarrier crosslinking reaction with 2mL of 50ug/ml laminin solution were taken immediately after addition of the laminin solution and after overnight incubation and its absorbance measured. For each sample, there were three replicates. The Bradford assay was performed following a protocol from Thermo Scientific [75]. Briefly, 150µL of each sample were added into 96-well plate (Corning). Then, 150µL of the dye was added to each well and mixed with a plate shaker for 30 seconds. The plate was removed from the shaker and left to incubate for 10min. at room temperature. The absorbance was measured at 595nm using a microplate reader (Infinite M200 Pro, Tecan). A laminin standard curve was prepared by measuring the values of absorbance of solutions with known concentrations of laminin in the range used in the functionalization experiments. Using the standard curve, it was determined the laminin concentration for each unknown sample.

2.3 Lt-NES cell culture

The lt-NES cell lines used in this work were derived from human ESC cell line I3 and maintained at passages P43-P49. Lt-NES were provided by the laboratory of Professor Oliver Brüstle (Institute of Reconstructive Neurobiology, Life and Brain Center, University of Bonn, Germany). Lt-NES were cultured

in a serum-free medium which consisted in DMEM/F12 (1:1) + Glutamax (Life Technologies) containing N2 supplement (1:100; Life Technologies), 1.6g/L additional glucose (Sigma), 0.2% additional human insulin (25mg/mL, Sigma), 100Umg/mL penicillin, 100µg/mL streptomycin (Life Technologies) and supplemented with 20ng/mL human EGF, 20ng/mL FGF-2 (both from Peprotech) and B27 (1:1000; Life Technologies. Cultures were maintained at 37°C under a 5% CO_2 humidified atmosphere.

2.3.1 Lt-NES cell thawing

Lt-NES cryopreserved in cryovials (Thermo Fisher) in liquid nitrogen were thawed in a 37°C water bath for a few seconds and ressuspended in 5mL of pre-warmed culture medium, followed by centrifugation at 1000 rotations per minute (rpm) for 3min. After removing the supernatant, the pellet was ressuspended in 2mL of culture medium supplemented with 20ng/mL EGF, 20ng/mL FGF-2 and B27 (1:1000) and plated onto poly-ornithine/ laminin coated 6well-plates (Corning). Briefly, culture vessels were incubated with 15µg/mL poly-ornithine at 37°C for at least 30min. Then, the vessels were washed with PBS, coated with 2µL/mL laminin solution in PBS and incubated at 37°C for at least 2 hours.

2.3.2 Lt-NES cell passaging

Cells were washed with PBS and incubated with Trypsin-EDTA (Life Technologies) for 5 mins in the incubator. Then, an equal volume of trypsin inhibitor (Life Technologies) was added as well as culture medium and cells were centrifuged at 1000rpm for 3min. The pellet was ressuspended in 5mL of culture media supplemented with 20ng/mL EGF, 20ng/mL FGF and B27 (1:1000) and viable cells were determined using the trypan blue (Life Technologies) exclusion method by counting in a hemocytometer under an optical microscope (Olympus). Cells were seeded at a density of 50 000 cells/cm^2 on poly-ornithine/laminin coated plastic dishes or T25 T-Flasks (Corning) before being seeded onto microcarriers. Culture medium supplemented with 20 ng/mL hEGF, 20 ng/mL FGF-2 and B27 (1:1000) was replaced every 2 days.

2.3.3 Lt-NES cell freezing

For cryopreservation, the cell suspension was centrifuged at 1000rpm for 3min and ressuspended in 90% culture media supplemented with 20ng/mL hEGF, 20ng/mL FGF and B27(1:1000) and 10% dimethyl sulfoxide (DMSO; Sigma), which is a cryoprotectant – prevents ice formation inside the cell. Then, were placed in a cryo-box (Nalgene) for controlled freezing at cooling rate -1°C per minute, and transferred to a -80°C freezer. After 24h, cells were transferred to liquid nitrogen at approximately -196°C for long term preservation.

2.3.4 Lt-NES cell expansion on microcarriers under static conditions

The adhesion and growth of lt-NES on different commercially-available microcarriers under static conditions were tested. Microcarriers were equilibrated in culture medium at 37°C before cell seeding. For each type of microcarrier an approximate area of 3cm^2 and an initial cell density of 5×10^4 cells/cm^2 were considered. A total number of 2×10^5 (or 6×10^5) cells were seeded onto the microcarriers in 24-well (or 6-well) ultra-low attachment plates (Corning) at 37°C. Culture medium was replaced every 2 days. Cell attachment and proliferation were assessed daily in the microscope (pictures were taken every two days). For each condition in 24-well ultra-low attachment plate, triplicates were analyzed. After 6 days, Lt-NES were detached from the beads with trypsin-EDTA and incubated at 37ºC for 7min. After trypsin inhibition, culture media was added and samples were filtrated using a cell strainer (Corning), in order to remove microcarriers. After centrifugation (1000rpm for 3min), cells were ressuspended in culture media supplemented with hEGF, FGF-2 and B27 and counted in a hemocytometer after trypan blue staining. To determine the maintenance of cell viability and morphology after microcarrier culture, cells were replated in poly-ornithine/laminin coated 24-well well-plates.

2.3.5 Lt-NES cell expansion on microcarriers under dynamic conditions

Cell culture under dynamic conditions was performed in spinner flasks with workings volumes of 30mL (StemSpan, Stem Cell Technologies). The spinner flask is equipped with an impeller with paddles and a magnetic stirring bar and it was placed over a magnetic stirring plate inside a CO_2 incubator, at 37°C.

Cells were cultured on Plastic and -COOH beads prepared as previously mentioned, both functionalized with 3µg/cm^2 laminin. Cells were previously expanded in static conditions (section 2.3) until confluence and inoculated as single cells at a final concentration of 9.4 x10^4 cells/cm^2, in a total of 10x10^6 cells. The final microcarrier concentration used was 10g/L, which corresponds to an equivalent area of 108cm^2 and 107 cm^2 for Plastic and COOH beads, respectively.

Cells mixed with microcarriers were incubated in a 6-well ultra-low attachment plate for 1.5 hours at 37°C in a CO_2 incubator, in approximately one third of the final volume of medium. Then, cells mixed with microcarriers were transferred to spinner flasks and incubated overnight with no agitation. The next day, continuous stirring was set to 25rpm and the final volume (30mL) was completed. After this period, continuous stirring was kept at 50rpm. Every day, half of the medium was replaced and growth factors (10ng/mL of FGF-2 and hEGF and B27 (1:1000)) were added. A static expansion control was performed to confirm the initial cell viability.

Duplicate samples of 500µL of the culture were collected from the spinner flasks on a daily basis. Samples were washed with PBS and incubated with trypsin-EDTA for 5 mins. at 37ªC to detach the cells from microcarriers. Trypsin inhibitor was added as well as culture medium and microcarriers were

removed by filtration, using a cell strainer. Cells were centrifuged at 1000rpm for 3min and the pellet was ressuspended in fresh culture media supplemented with the growth factors. Viable cells were determined by counting in a hemocytometer using the trypan blue exclusion method under an optical microscope. Fold increase in cell number was calculated as the ratio between the cell number at the end of culture and the initial inoculated cell number.

2.3.5.1 Analysis of metabolites and nutrients in culture medium

In order to determine the concentration of glucose and lactate in the culture medium, samples were collected from the spinner flask culture. Microcarriers were allowed to settle and supernatant was centrifuged at 1500rpm for 10mins and kept at -20°C for subsequent analysis. An automatic analyzer (YSI 7100MBS, Yellow Springs Instruments) was used to determine the glucose and lactate concentrations present on the culture medium collected throughout the culture. Specific lactate production rate (q_{lac}) and specific glucose consumption rate (q_{gluc}) were calculated according to equation 1:

$$q = \frac{\Delta C}{\bar{X}\Delta t} \quad (1)$$

Where ΔC is the lactate produced/ glucose consumed during the time period Δt and $\bar{X}$ is the average number of cells in culture during the same period. The apparent lactate from glucose ($Y_{lac/gluc}$) yield was calculated as the ratio between q_{lac} and q_{gluc}.

2.4 Lt-NES cell characterization

2.4.1 Immunocytochemistry

Expression of NSC and neuronal differentiation markers were accessed by immunocytochemistry, after static and dynamic cultures. In order to stain the cells, the following protocol was applied. Cells on culture plates were fixed with 4% paraformaldehyde (PFA) solution (Sigma) for 10 mins. at room temperature and washed with PBS to remove the fixation agent. Next, cells were permeabilized with blocking solution 10% FCS (Life Technologies), 0,1% Triton X-100 (Sigma) in PBS for 30-60min. at room temperature. Blocking solution was aspirated and cells were incubated overnight at 4°C with primary antibodies diluted in staining solution (5% FCS, 0,1% Triton X-100 in PBS). After the incubation period, cells were washed with PBS and incubated with the appropriate secondary antibody conjugated to Alexa fluorophores for 1h at room temperature, protected from light. After washing with PBS, nuclear DNA was stained with DAPI (Sigma), dilution 1:10000, for 2 minutes at room temperature. Cells were washed and analyzed under a fluorescence microscope (Leica DMI 3000B). The antibodies used are described in the *Tables 3* and *Table 4*.

Table 3: Primary antibodies and respective dilutions used in immunochemistry assays.

Primary Antibodies			
Target	**Host**	**Source**	**Dilution**
Nestin	Mouse IgG	R&D Systems	1:200
Sox2	Mouse IgG	R&D Systems	1:500
TUJ1	Mouse IgG	Covance	1:4000

Table 4: Secondary antibody used in immunocytochemistry assays.

Secondary Antibodies			
Target	**Host**	**Source**	**Dilution**
Alexa 546	goat anti-mouse IgG	Life Technologies	1:500

2.5 Statistical Analysis

The results presented are expressed as mean ± standard error of the mean (SEM), displayed as the error bars:

$$SEM = \frac{\sigma}{\sqrt{n}} \quad (2)$$

Where *n* is the number of samples.

3 Results and Discussion

3.1 Validation of the EDC/sulfo-NHS crosslinking in surface conjugation

Polystyrene microcarriers with COOH or NH_2 groups on the surface were functionalized with laminin through EDC/sulfo-NHS crosslinking. In the presence of sulfo-NHS, EDC can be used to activate carboxylic groups, allowing for the formation of an amide bond between a protein and the microcarrier. The rationale to conjugate laminin to the beads through crosslinking instead of adsorption relies on the higher stability of covalent bonds compared to a coating based on passive adsorption. Therefore, covalent bonds would be more resistant to the shear forces present in stirring environments, minimizing the release of cells from the microcarriers.

In order to validate the occurrence of the covalent coupling reaction and quantify the amount of protein attached to the surface of the beads the Bradford colorimetric method was used due to its simplicity, rapidity and sensitivity. The Bradford method relies on proportional binding of the dye Coomassie blue to the protein, thus, the more protein present, the more dye binds to it. Samples were taken right after the addition of the laminin solution to the beads and after overnight reaction period. The concentration of the protein on the samples was estimated by comparing its absorbance with a standard curve, obtained from a series of solutions with known concentrations of laminin. In general, bovine serum albumin (BSA) is used to prepare the standard curve for the Bradford assay, however, for more accurate results, the standard curve should be prepared from a pure sample of the target protein to be measured, in this case, laminin. Supernatants of laminin-adsorbed microcarriers were also read in order to compare efficiencies of both coupling procedures. A decrease in the absorbance of the supernatants taken after the incubation period of both coupling reactions is expected since the attachment of laminin to the beads would cause a reduction in its concentration in the supernatant of the reaction mixtures.

As it can be seen in *Figure 10,* it is observed a decrease, although slight, in the absorbance of the condition of the EDC/NHS reaction. A small reduction is also observed for the adsorption condition. No difference in the absorbance was observed when no protein was present in the supernatant. As expected, the initial value of the sample of supernatant beads without laminin sample is lower than the value of the initial absorbance of both coupling mixtures.

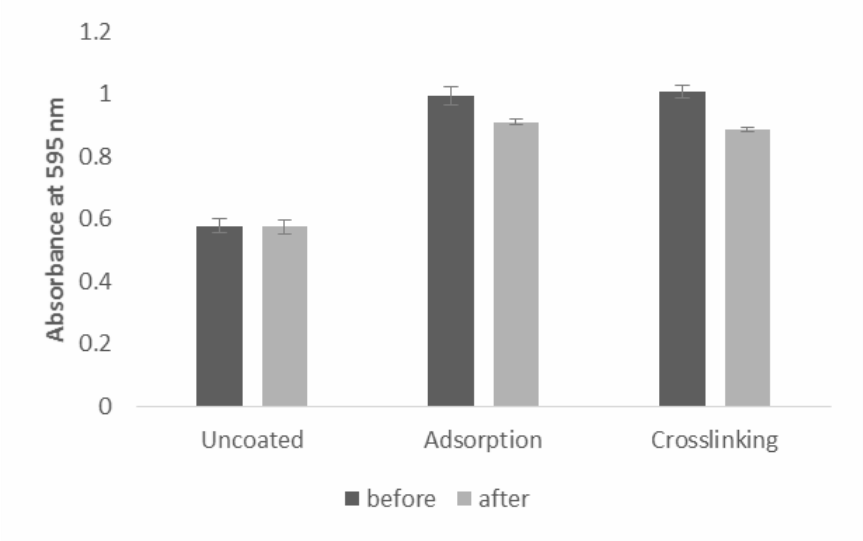

Figure 10: Absorbance of supernatant samples of laminin crosslinked beads, measured right before and after the incubation period of the reaction. Absorbance of uncoated beads (blank) and laminin adsorbed beads were measured at the same time periods. Results of crosslinking are the average of 3 independent experiments, uncoated and adsorption are the average of 2 independent experiments. Error bars represent SEM.

Using the laminin standard curve (*Figure 11*), obtained after the plotting of the laminin absorbance measurements for each dilution versus its concentration (µg/mL), the concentration of laminin in the supernatant samples was estimated. Calculations were then performed to determine the amount of protein that did not conjugate to the beads. The results are presented in *Table 5.*

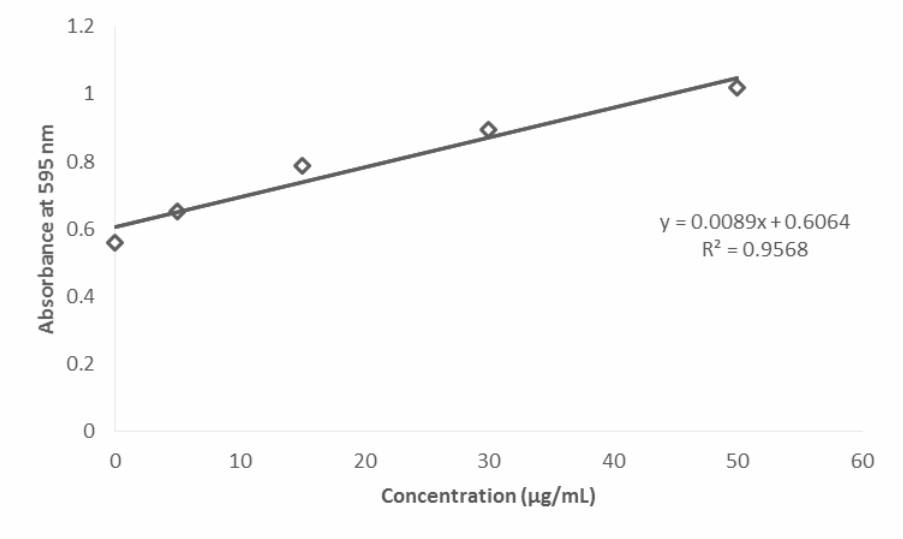

Figure 11: Laminin calibration curve

Both reactions had similar behaviors: the final concentration of protein and respective mass in supernatant samples were lower than the initial values. Covalent bonding showed to be slightly better in protein immobilization, having a protein attachment efficiency of 45% against the 41% achieved by the adsorption.

Table 5*:* Laminin **c**oncentration and mass present in the supernatant samples of crosslinked beads and coupled through adsorption, and protein attachment efficiency of the respective coating procedures. Initial: Before the incubation period; Final: after the incubation period.

Coating procedures	Concentration (µg/mL)		Mass (µg)		Protein Attachment Efficiency (%)
	Initial	Final	Initial	Final	
Adsorption	43.4	34.0	86.8	51.1	41
Crosslinking	43.5	31.9	87.1	47.9	45

Despite the small difference in the efficiencies of both methods, the higher efficiency of the crosslinking reaction is in agreement with the literature. Junka *et al* showed that EDC-crosslinked laminin scaffolds presented a higher amount of laminin on the surface when compared to laminin adsorbed scaffolds or uncoated scaffolds [76].

The difference between the theoretical amount of laminin added into the reaction mixture (100 µg) and the initial masses calculated based on the initial concentration portrays the error of the Bradford assay in laminin absorbance measurement due to its low specificity to the protein. Considering the theoretical amount of the protein added into the sample of 15mg of beads (5.4cm^2), the amount of laminin attached to the beads after the EDC/sulfo-NHS crosslinking is 52.1µg, which corresponds to a concentration of 9.6µg/cm^2. Likewise, for the beads coupled through adsorption, the amount of protein attached is 48.9µg, corresponding to a concentration of 9.1 µg/cm^2. Thus, such differences of both methods in protein attached per bead are irrelevant.

The small differences in the absorbance values of the “before” and “after” readings and the apparent low efficiencies of the reactions may be due to the low color variation of the dye of the Bradford assay to laminin. The Bradford dye exhibits a wide color variation response to different individual proteins, which can be confirmed when comparing the dye response curves to BSA, used as the common standard, and to laminin (*Figure 12*) [77]. The development of color of the Bradford assay varies between different proteins since it depends mainly on certain amino acids present in the protein’s sequence, the isoelectric point, secondary structure and the presence of specific side chains or prosthetic groups. Therefore, a more accurate and specific method would be needed to validate the crosslinking reaction and quantify the amount of laminin available at the surface of the beads. In another study [54], the covalent attachment of Matrigel by EDC/NHS to PCL scaffolds was also assessed by two different methodologies: the morphology of the scaffolds was studied by scanning electron microscopy and the surface chemistry by infrared spectroscopy. The latter confirmed the occurrence of the covalent attachment of the matrix on the

surface of the scaffolds [54]. However, such methods provided only qualitative information regarding scaffold functionalization. Similarly, infrared spectroscopy was performed in the context of this work without conclusive results (results not shown).

The efficiency of the crosslinking reaction could probably be slightly improved by optimizing the protocol. For instance, according to the protocol described by Hermanson et al [61], in an EDC/NHS reaction the protein to be conjugated to the beads should be dissolved at a concentration of 1- to 10-fold molar excess over the concentration of the functional groups. Given that the carboxyl beads used have a carboxyl group capacity of 2.01mmol/g, to achieve at least an equal concentration of laminin that should be dissolved, it was necessary an approximate amount of 24g, which, however, is not feasible due to the protein costs.

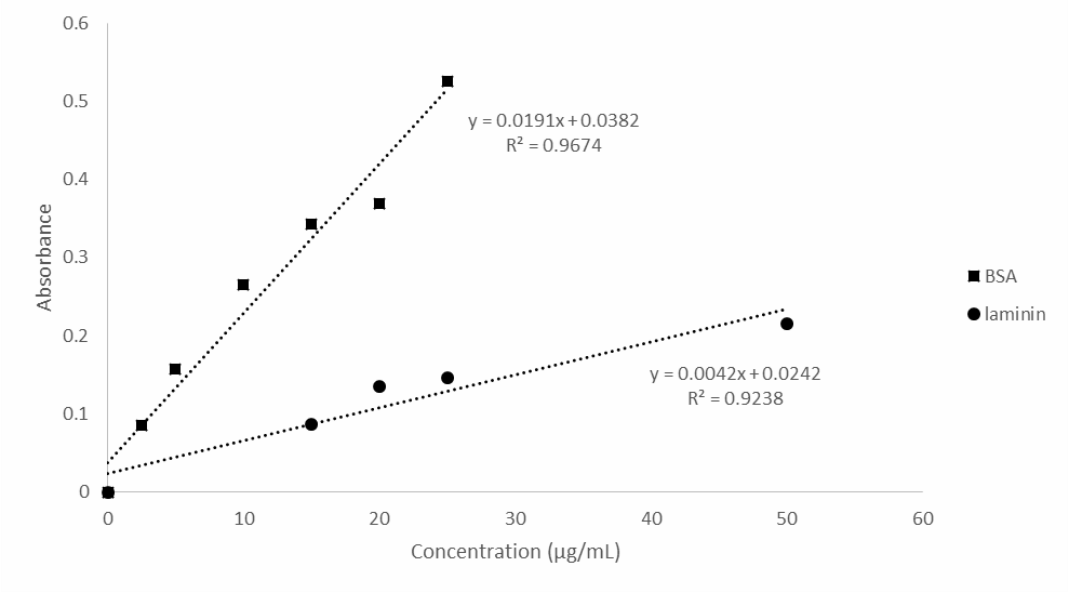

Figure 12: Comparison of BSA and laminin standard curves

Given the previous data, quantification of laminin is not conclusive due to the low color yield of the Bradford dye to the protein. Moreover, it appears that covalent bonding does not result in a considerably higher amount of protein attached to the surface of the microcarriers as compared to physical adsorption. The hypothetical advantage of covalent bonding in stirring environments to stabilize protein attachment will be assessed in posterior sections. It would be also valuable to test the stability of protein immobilization when crosslinked to the beads to assess the off-the-shelf potentiality of the system.

3.2 Lt-NES cell culture under static conditions

Successful cultures of lt-NES in static conditions using two dimensional surfaces have already been described in the literature [16, 17]. In order to scale-up the culture of lt-NES, which are anchorage-

dependent cells, adequate substrates are required that efficiently support cell attachment and proliferation in suspension cultures under dynamic conditions.

For this purpose, a first screening of different commercially available microcarriers was performed in static conditions with different surface functionalization techniques and coatings. The performance of Plastic, Cytodex 1 and Cytodex 3 microcarriers with a poly-ornithine/laminin adsorption coating was assessed, as well –COOH and -ÑH$_2$ microcarriers with laminin covalently attached. Moreover, since Plastic beads have no surface charge, a coating only with poly-ornithine, a cationic compound, was also considered in order to evaluate if charging is sufficient to promote cell attachment and growth. Throughout the culture, important aspects such as cell attachment, proliferation, the presence of cell clusters, either in suspension or on the microcarrier surface and microcarrier agglomeration due to cell "bridging" were monitored daily by visual inspection (*Figures 13* and *14*, *Table 6*).

Table 6: Qualitative assessment of attachment and survival of cells, occurrence of free cell aggregates in the medium and bead aggregation due to cell "bridging" in the different types of coated microcarriers and respective controls.

Type of microcarrier	Coating	Attachment	Proliferation	Cell aggregates	Microcarrier agglomeration
Plastic	None	Poor	Medium	Occasionally	No
	PO	Medium	Medium	Yes	No
	PO+LN	Good	Good	No	Yes
Polystyrene AM NH_2	None	Medium	Good	Yes	No
	LN	Medium	Medium	Yes	No
Carboxy polystyrene	None	Poor	Medium	Occasionally	No
	LN	Good	Good	Occasionally	Occasionally
Cytodex 1	None	Poor	Poor	No	No
	PO+LN	Medium	Good	No	Yes
Cytodex 3	None	Poor	Poor	No	No
	PO+LN	Poor	Poor	No	No

Due to the poor attachment and survival of cells with Cytodex 3 and with uncoated Cytodex 1 these were not consider in the following studies (*Figure 14 A,C,D*). Also, since with –NH_2 microcarriers, even when conjugated with laminin, cells did not proliferate as monolayers on microcarriers, these were not also used in subsequent experiments (*Figure 13 D, E*).

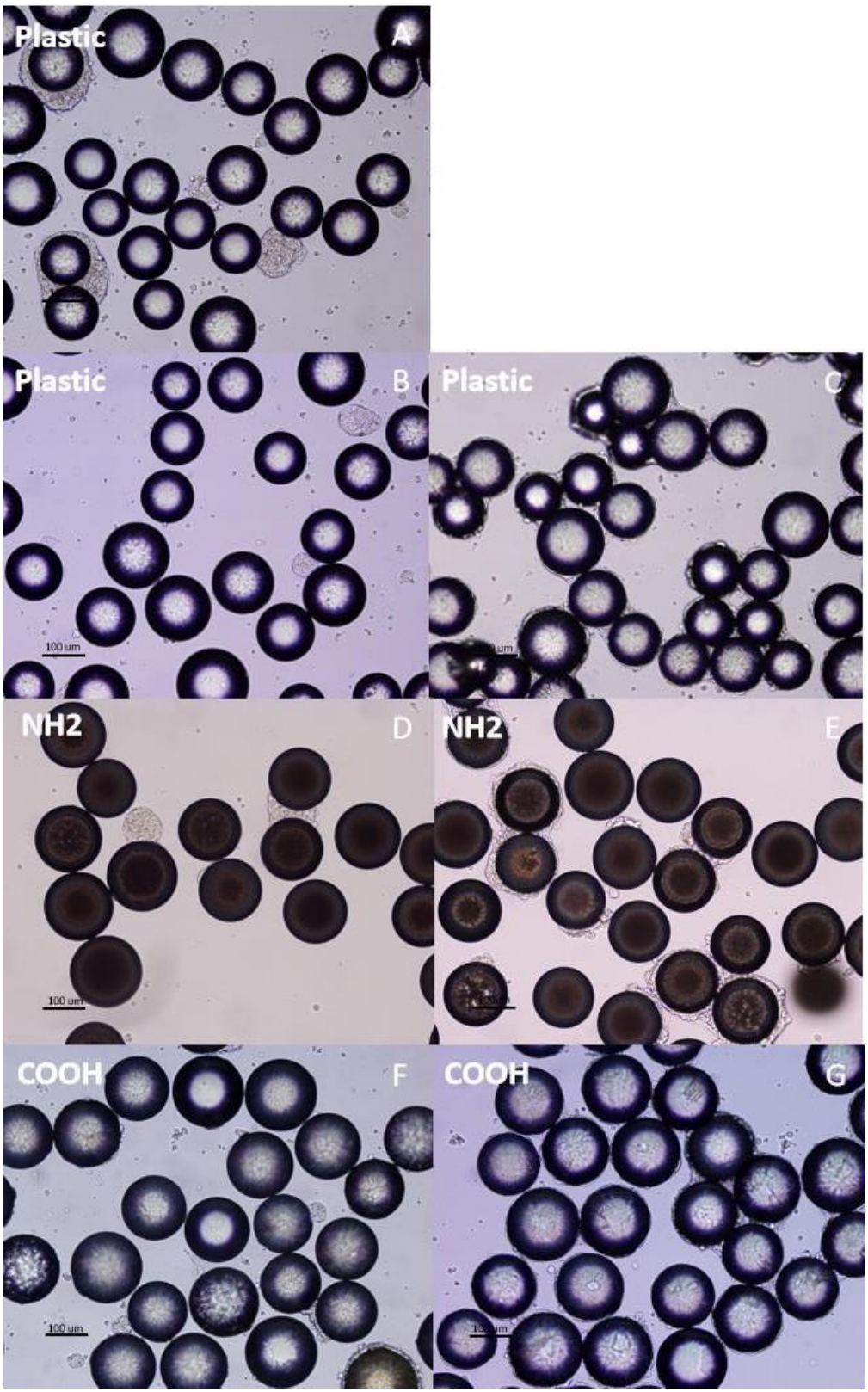

Figure 13: lt-NES culture in day 5, under static conditions, in uncoated microcarriers (A,D,F), poly-ornithine coated microcarriers (B), poly-ornithine/laminin coated microcarriers (C) and laminin crosslinked microcarriers (E,G)

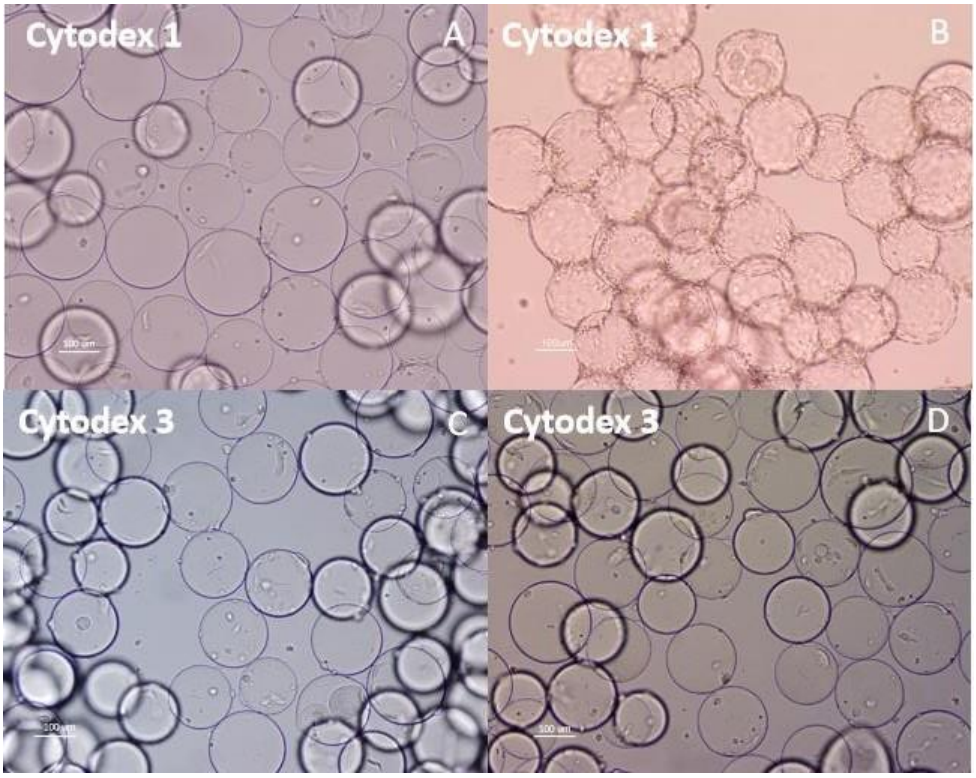

Figure 14: lt-NES culture in day 5, under static conditions, in uncoated (A,C) and poly-ornithine/laminin coated Cytodex 1 and Cytodex 3 (B,D)

For the conditions with better results, cell counts were performed after six days of culture and the results, as well as the fold increase in cell number, are shown in *Figure 15.* Plastic microcarriers coated only with poly-ornithine showed no significant improvement in cell growth compared to the uncoated conditions (*Figure 15*). In addition, after a few days, small clumps of cells were observed in suspension in the culture medium or attached to the beads (*Figure 13 B*). On the other hand, poly-ornithine/laminin coated Plastic microcarriers provided the best result in terms of cell expansion, with visible spreading of cells on the microcarriers´ surface and cell "bridging" between beads (*Figure 13 C*). Cell expansion was also higher than observed with Cytodex 1, even with the same coating (*Figure 15*).

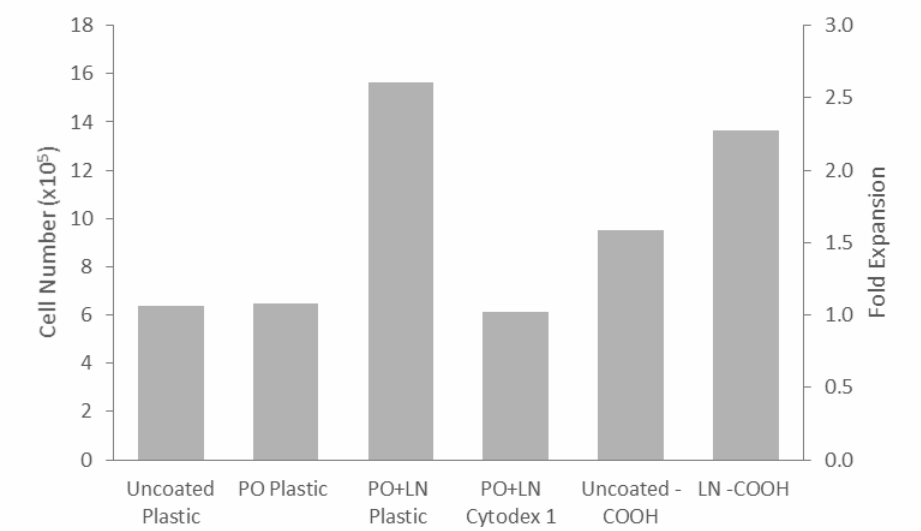

Figure 15: Cell number and fold expansion after 6 days of culture in Plastic, Cytodex 1 and –COOH beads under static conditions. PO: poly-ornithine; LN: laminin. Results of one experiment.

Positively charged surfaces are known to promote for rapid cell adhesion but are often not sufficient to sustain cell growth given the nonspecific physical interactions between the surfaces and the cells [47]. This seems to be the case for the poly-ornithine coated Plastic beads, explaining the low cell number observed after 6 days of culture. Another possible explanation could be related with excessive electrostatic charge, which could be inhibiting cell spreading and growth [78]. Such effect may also be translated to Cytodex 1, since the microcarrier is naturally positive given the charged groups and was additionally coated with poly-ornithine. The results obtained with poly-ornithine Plastic suggest that a poly-ornithine coating is not enough to support the attachment of lt-NES, leading to the formation of cell aggregates in suspension, and thus has not a beneficial effect in relation to the uncoated beads. In contrast, poly-ornithine/laminin coated Plastic beads promoted good cell attachment to the beads surface (*Figure 13 C*), with few free clumps of cells in suspension probably due to the combination of the electrostatic interactions promoted by the positively charged poly-ornithine and the signaling pathways for attachment triggered by the ECM adhesion protein laminin. These surface features are more appropriate for cell spreading and cell growth, which explains the better results.

Carboxyl beads conjugated with laminin exhibited a higher cell-fold expansion compared with the non-conjugated beads (*Figure 15*). Confluent microcarriers were visible at the microscope, after a few days of culture, with only residual free cells in medium (*Figure 13 C*). Therefore, surface conjugation of –COOH beads by EDC/sulfo-NHS was effective in the enhancement of cell attachment and growth. Curiously, non-conjugated beads performed better than expected since surfaces presenting carboxylic groups are cell repellent due to reduction in their wettability [79]. The establishment of an optimized system for lt-NES cell culture will depend on extensive studies focused on cell adhesion and proliferation on different materials and coating layers.

Lt-NES from poly-ornithine/laminin adsorbed plastic and Cytodex 1 and –COOH conjugated beads were then evaluated regarding their viability and phenotype. Cells were replated in poly-ornithine/laminin dishes, where they continued to proliferate and maintained their neural rosette-like growth pattern (*Figure 16*). The expression of specific markers was assessed by immunocytochemistry (*Figures 17,18, 19*). Cells from the experiments expressed Nestin and Sox 2, which are markers of neural progenitor/stem cells, and occasionally βIII-tubulin (Tuj1), associated with spontaneous neuronal differentiation which is expected [16].

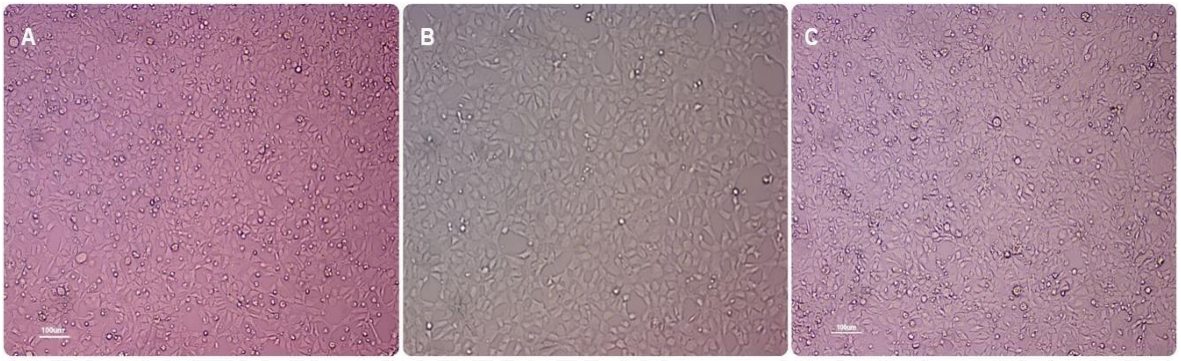

Figure 16: lt-NES harvested from laminin conjugated carboxyl (A), poly-ornithine/laminin adsorbed Cytodex 1 (B) and Plastic (C) microcarriers and replated in poly-ornithine/laminin tissue culture plates**.**

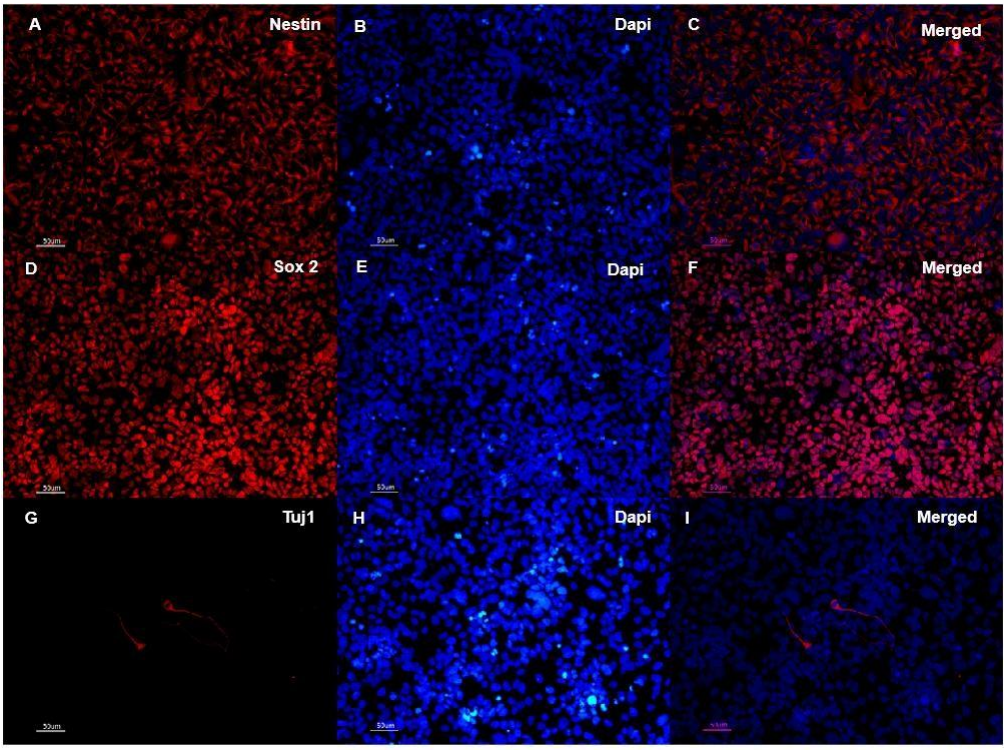

Figure 17: Immunostaining of cells for NSC markers Nestin (A-C), Sox 2 (D-F) and neuronal differentiation marker Tuj1 (G-I) expression after culture in poly-ornithine/laminin adsorbed Plastic microcarriers under static conditions.

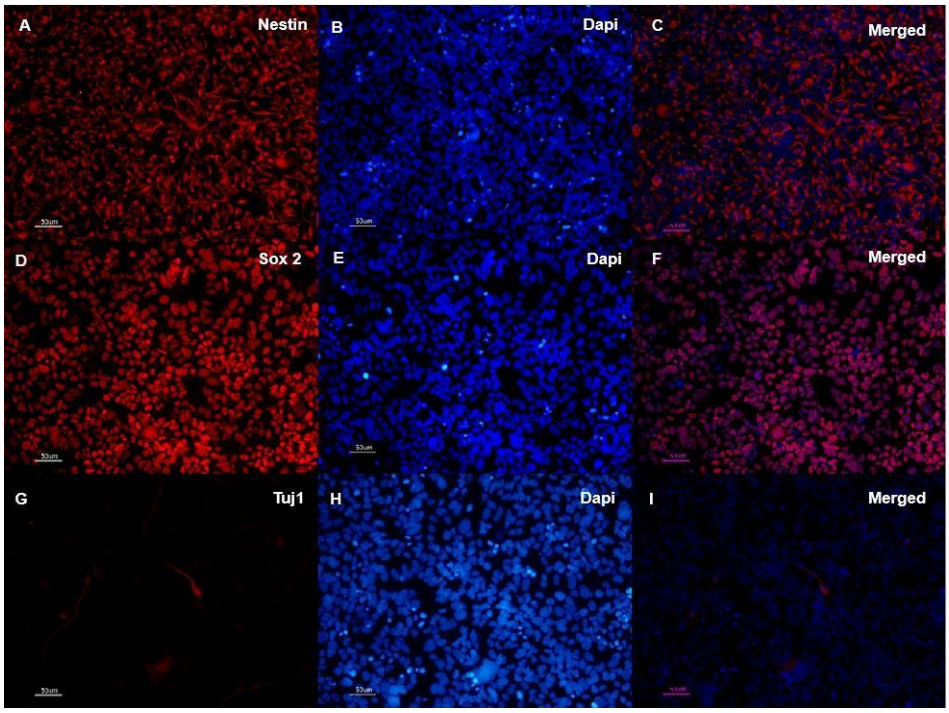

Figure 18: Immunostaining of cells for NSC markers Nestin (A-C), Sox 2 (D-F) and neuronal differentiation marker Tuj1(G-I) expression after culture in laminin conjugated –COOH microcarriers under static conditions.

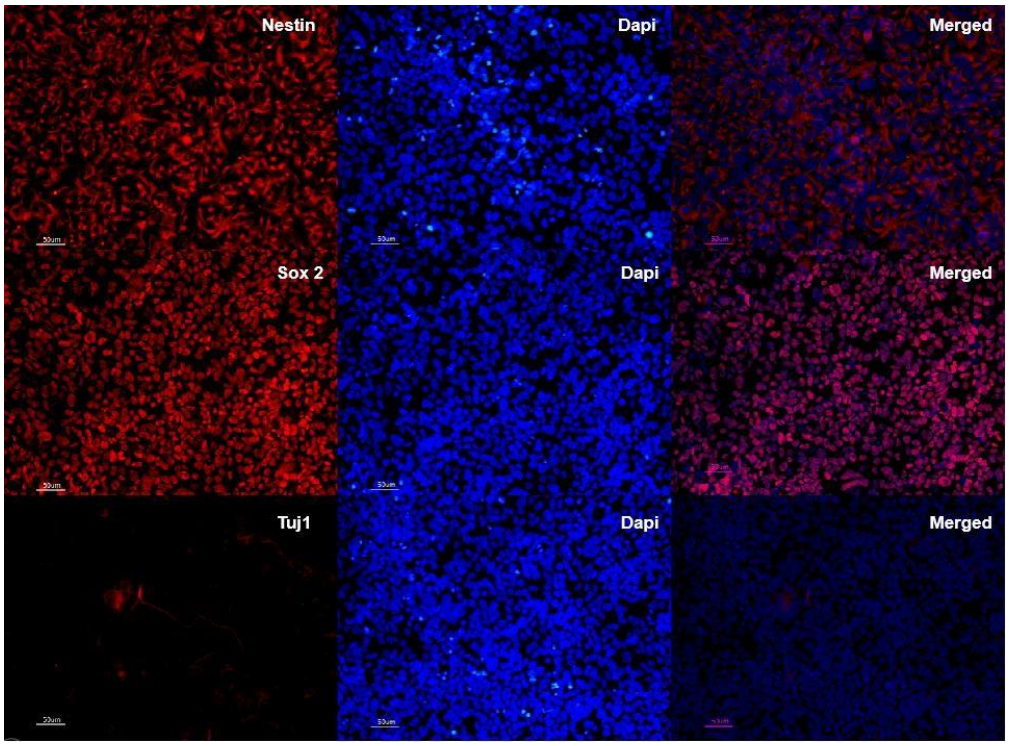

Figure 19: Immunostaining of cells for NSC markers Nestin (A-C), Sox 2 (D-F) and neuronal differentiation marker Tuj1 (G-I) expression after Cytodex 1 culture under static conditions.

Given these results, it was concluded that Plastic microcarriers coated with poly-ornithine/laminin and –COOH microcarriers with laminin covalently bound support lt-NES attachment and growth, with maintenance of NSC identity after re-plating. Moreover, the results depict the versatility of lt-NES to be cultured in microcarriers made of different materials. However, optimization of cultures is fundamental to efficiently scale-up and that was the drive for the next section of the present work.

3.2.1 Comparison of adsorbed and crosslinked microcarriers

Prior to spinner flask culture, different concentrations of laminin were tested to determine the optimal coating conditions, either by adsorption or EDC/NHS crosslinking, for lt-NES culture. Cytodex 1 and Plastic microcarriers were coated through adsorption with both poly-ornithine and laminin, according to the previous results. The laminin coating concentration suggested by the Plastic beads manufacturer (Pall/Solo Hill) is 1-10µg/cm^2, so the concentrations were chosen to be within that interval. Carboxyl microcarriers were conjugated via EDC/sulfo-NHS reaction with the same laminin concentrations used in the adsorbed microcarriers for comparison. Since –COOH group concentration was constant in the Carboxyl microcarriers (2.01mmol/g), it was hypothesized that protein conjugated to the beads would be proportional to the protein used in the coupling reaction.

Lt-NES cultures were followed for 6 days, being the culture morphology assessed daily by light microscopy and cells were counted after that period. The highest cells numbers were obtained with the covalent bounded beads, all of them being superior to their adsorbed counterparts (*Figure 20*). The highest cells yields were achieved with 2µg/cm^2 –COOH beads. Comparing the different types of microcarriers in the same conditions, it is visible that Cytodex 1 was the one with the lowest performance and -COOH beads had slightly better results than plastic. Regarding the adsorbed beads, 3µg/cm^2 plastic condition was superior to all of the other conditions. Apparently, there is no proportional relation between the amount of laminin coated and the number of cells: 2 and 1µg/cm^2 concentrations gave similar results for plastic beads, 2µg/cm^2 was superior to 3µg/cm^2 for –COOH microcarriers.

Aggregation of beads and “cell bridging”, probably due to the absence of agitation, were observed in all of the conditions, with the exception of all experiments with laminin crosslinked carboxyl beads, after a few days of culture (*Figures 21 and 22*). That has been shown to be detrimental to cell expansion as a result of limitations in the diffusion of oxygen and nutrients that may lead to necrotic centers inside the cell/microcarrier aggregates [80]. Initial agitation in static conditions could potentially diminish bead agglomeration and enhance cell adhesion by preventing cell aggregation, since aggregates are less likely to adhere to the beads.

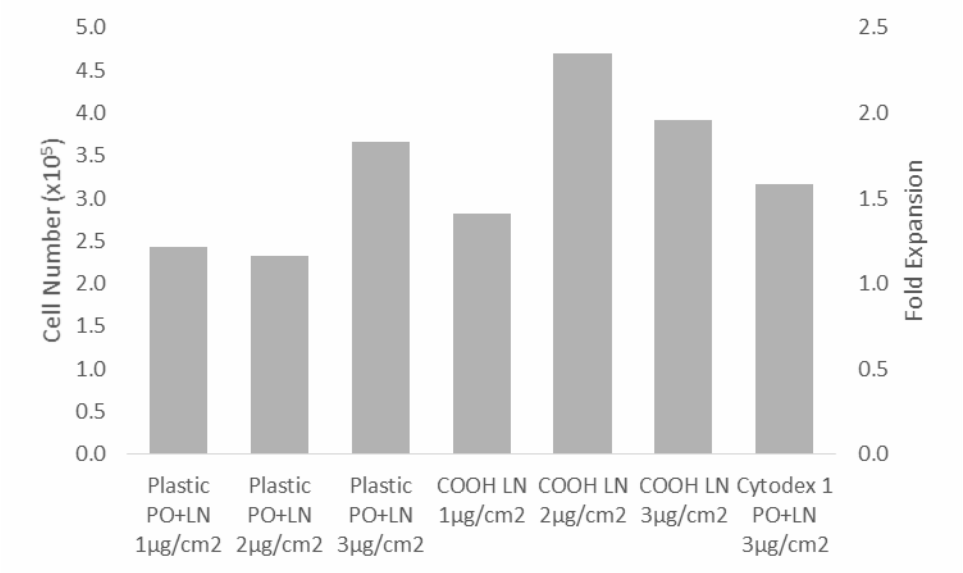

Figure 20: Cell numbers after 6 days of culture in adsorbed Plastic and Cytodex 1 beads and conjugated -COOH beads, with different laminin concentrations. Results of one experiment.

Although the 2µg/cm^2 laminin crosslinked –COOH beads gave slightly better results regarding cell number, the same concentration of the protein was shown to be suboptimal for the adsorption condition. It is important to note, though, that the experiment was performed only once and the difference may be within the experimental error. However, to compare the performance of the adsorbed and crosslinked beads in spinner flask cultures, it was decided to choose an identical laminin concentration for both methods. Given the previous results, poly-ornithine coated Plastic microcarriers and –COOH microcarriers, both conjugated with 3µg/cm^2 of laminin, were chosen to be compared for the culture of lt-NES cells in spinner flasks, since this concentration was one of the best for both methods.

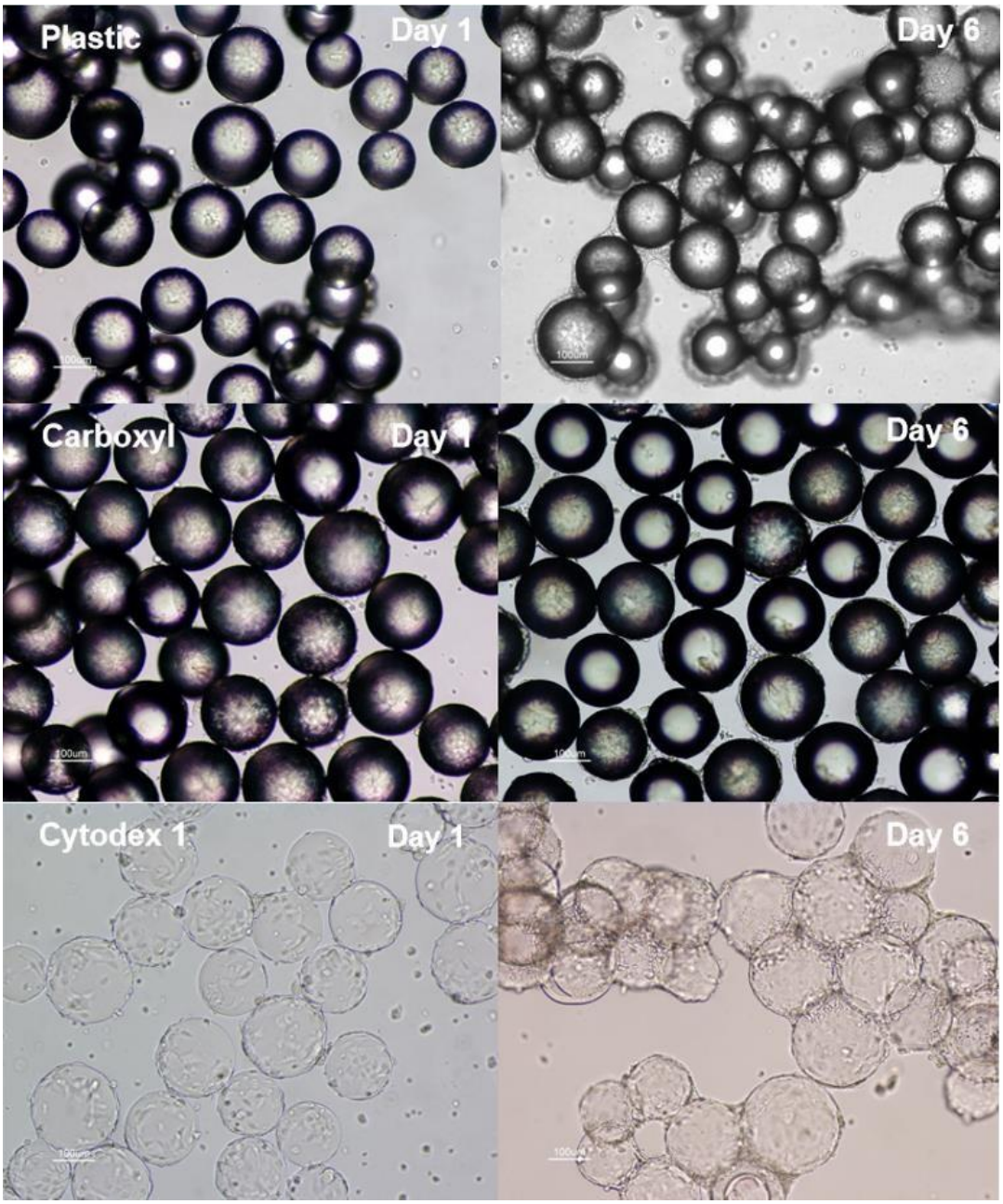

Figure 21: Bead aggregation evolution under static conditions in poly-ornithine + laminin 3µg/cm^2 Plastic, Cytodex 1 beads and, laminin 3µg/cm^2 Carboxyl.

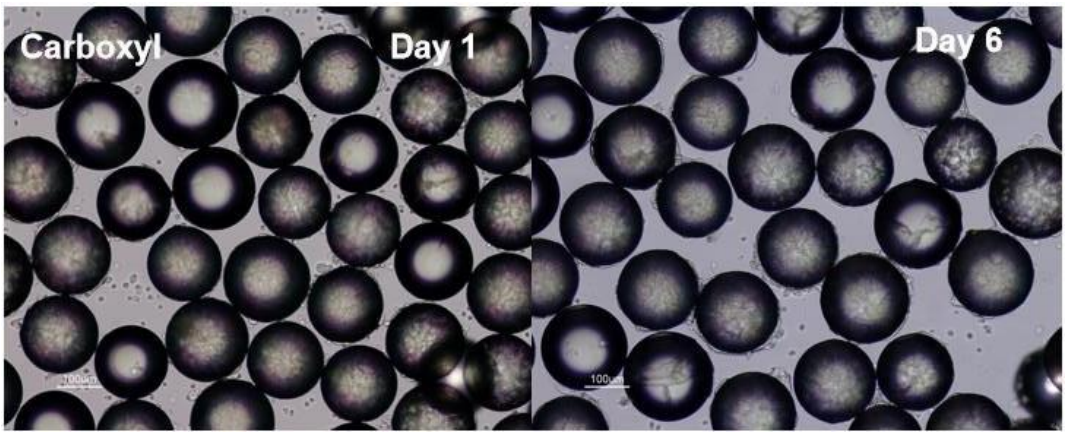

Figure 22: Bead aggregation evolution under static conditions in laminin 2µg/cm^2 Carboxyl microcarriers

3.3 Lt-NES cell culture under dynamic conditions

Envisaging the development of a large-scale bioprocess for lt-NES cell production, the results and conclusions already described were used to perform a preliminary experiment in dynamic culture conditions, using spinner flasks as model bioreactors. It is important to note that hydrodynamic conditions of a spinner flask differ from the conditions of a bioreactor and also that a spinner flask lacks online monitoring and feedback loop control of important variables (O_2, pH). Nonetheless, this set up allows the study of the effect of agitation by stirring and pH and O_2 is controlled by incubation of the culture system. An initial concentration of 10g/L of microcarriers, which corresponds approximately to an equivalent surface area of 108cm^2, was used, and 10x10^6 cells were seeded. A concentration of 3µg/cm^2 of laminin was used to coat the microcarriers. In the first 24h, microcarriers were suspended in 10mL, 1/3 of the final volume (30mL) to increase the frequency of cell- -bead interactions, improving cell attachment, as well as to concentrate the autocrine factors released by the cells. Agitation was only applied after 24h to promote an adequate environment for the cells to attach the beads. Cell growth was assessed by daily cell counts and analysis of the concentration profile of the nutrient glucose and the metabolite lactate. The cells were replated in static conditions after a few days of expansion and in the end of the plastic spinner flask culture, the expression of Nestin, Sox 2 and Tuj1 was verified by immunocytochemistry.

3.3.1 Caboxyl microcarrier culture in spinner flask

Given the promising results obtained with laminin crosslinked beads in static, the system was translated to a spinner flask. As it can be seen in *Figure 23*, culture was only kept for five days since cell survival reduced throughout the culture period and no fold increase in cell number was registered. Agitation was started in day 1 and increased in day two, being the lowest point of the culture registered the next day,

which indicates optimum values for agitation speed were not applied. Adhesion of cells onto the beads and overall homogeneous occupancy was visible in days one and two, but extensive detachment followed afterwards with cell clumps being observed in the medium (*Figure 24*).

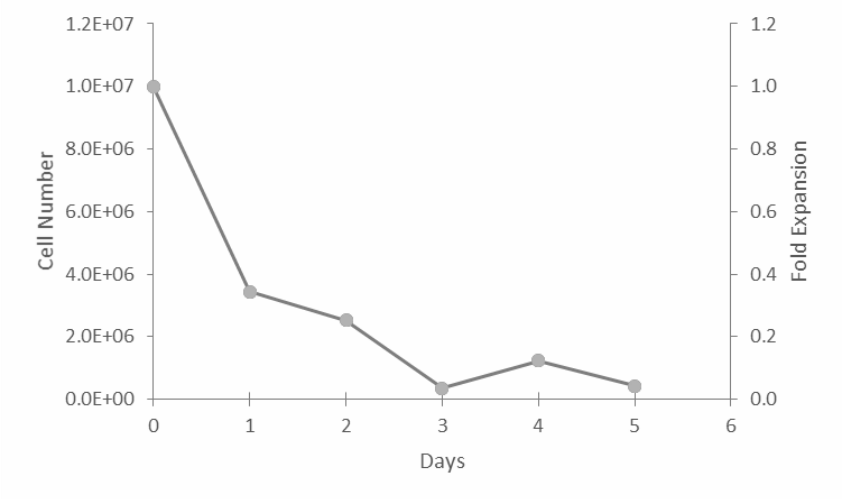

Figure 23: Growth curve of lt-NES cultured in spinner flasks with 3µg/cm^2 laminin crosslinked –COOH beads. Results of one experiment.

It must be pointed out that, although the microcarrier weight used was the same for both spinners (300mg), it was clear a reduction in the quantity of the –COOH microcarriers after the laminin immobilization steps. This reduction could be due to loss of particles explained by the high number of washing steps that those had to be subjected to, given the EDC/NHS reaction protocol. It was also observed that these had a higher sedimentation speed, being less prone to stay in suspension than the Plastic microcarriers, despite having the same density.

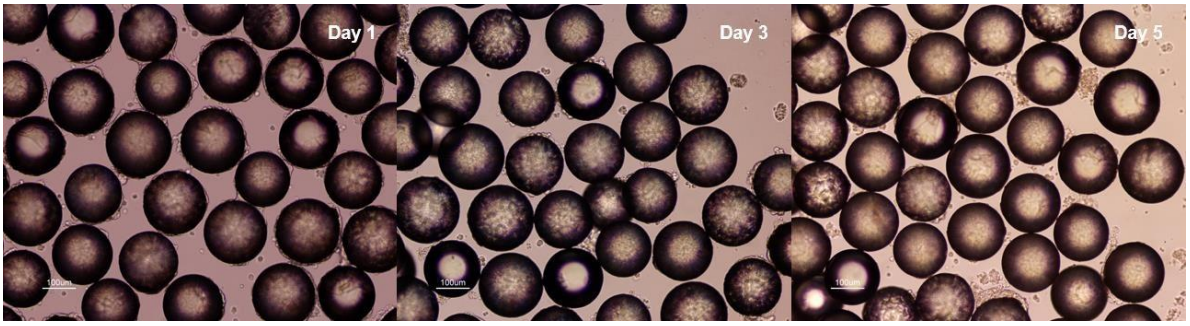

Figure 24: lt-NES cell occupancy on –COOH beads harvested in day 1, 3 and day 5 of culture in spinner flask.

Unsuccessful scale up using this same system is reported in the literature: despite –COOH conjugated beads supported hPSCs growth in static cultures, extensive detachment was observed under stirring conditions [58]. It is hypothesized that adhesion of cells in this type of system is not strong enough to prevent detachment under stirring. As future work, additional conjugation of the –COOH beads with pLL

adsorption, a synthetic cationic polymer that enhances cell attachment and promotes the adsorption of ECM proteins, could circumvent this problem, as it is described as well by Fan *et al*. [58]. Seeding efficiency and growth may also be increased with the optimization of laminin attached to the microcarriers' surface. For this purpose, optimization of the coating procedures will also be fundamental.

The combination of all of the previous factors may explain the failure of laminin crosslinked carboxyl beads in lt-NES culture under dynamic conditions. A less amount of beads resulted in less surface available for adhesion, that together with the weak cell adhesion forces in an agitated environment led to detachment and poor survival.

Levels of glucose and lactate were evaluated throughout spinner flask culture. Half of the medium was refreshed every day, thus, metabolites such as lactate and ammonia are partially removed from culture, and glucose is replaced. Glucose is one of the main sources of energy and carbon for cell metabolism. Based on *Figure 25,* no significant glucose consumption rates were observed, which is consistent with the low cell number and cell death, being only noticeable a slight reduction in concentration in the first days of culture when a higher number of cells was counted. As for lactate, it is produced typically in exponential growth phase resulting from cells metabolism and its accumulation in the culture medium lowers the pH, which can be harmful to the cells [67]. Values of inhibitory concentrations were reported for some types of stem cells (16mM for rat mesenchymal stem cells, or 35.4mM for human mesenchymal stem cells) [81]. The lactate concentrations registered were below those values, reaching a maximum value of 9.16mM, thus, theoretically, lactate accumulation did not had toxic effects in the system. A reduction of lactate levels occurs from day 3 until the end of culture, corresponding to the lowest cell numbers reached in the culture. The average molar ratio of lactate produced over glucose consumption $Y_{lac/gluc}$ was 1.91, which is approximate to the maximum theoretical value of 2, correspondent to the glucose metabolism by anaerobic glycolysis [82]. Therefore, approximately 2 moles of lactate per 1 mole of glucose were produced.

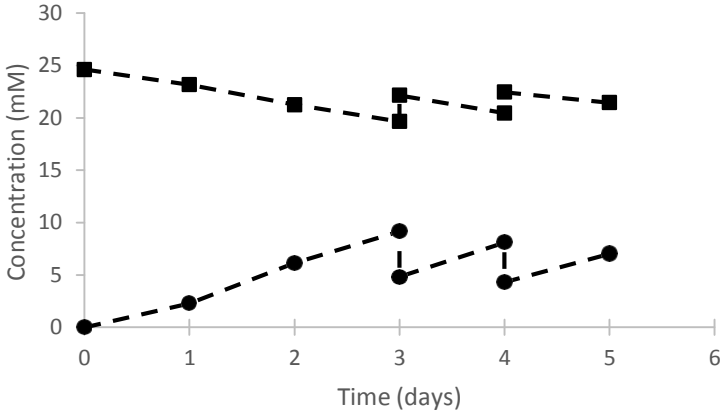

Figure 25: Concentration profile of glucose (■) and lactate (●), in mM, during lt-NES -COOH beads culture in spinner flask. Results of one experiment.

Given the present data, it may be concluded that results obtained in static microcarrier cultures cannot be directly translated to dynamic environments. Laminin crosslinked –COOH beads efficiently supported lt-NES cell attachment and growth in tissue culture plates, but were not capable to do so when cultured under dynamic conditions in a spinner flask. Future work should include the additional pLL coating to the carboxyl beads and compare them alongside with adsorbed beads in stirring environments with optimized culture parameters, including microcarrier concentration or cell inoculation density, agitation schemes and speeds.

3.3.2 Plastic microcarrier culture in spinner flask

Simultaneously to the carboxyl beads spinner flask culture, a 3µg/cm^2 laminin and poly-ornithine adsorbed Plastic microcarrier spinner flask was also performed. The growth curve is depicted in *Figure 26* and growth parameters are shown in *Table 7,* with the exception of specific growth rate and duplication time. The latter could not be calculated since no exponential growth phase is clearly identifiable in *Figure 26*. At day 1 of culture, about 60% of the inoculated cells adhered to the plastic beads, corresponding to almost twice the value for carboxyl beads, which presented 34% of seeding efficiency. At the end of culture, the spinner flask promoted a fold expansion of 1.54 in cell number, with a maximum of 1.69 detected at day 9. In addition, adherent cells exhibited a 2.5-fold increase in cell number.

Table 7: Growth parameters of lt-NES cultured in spinner, adherent to plastic beads. Fold expansion relates to to expansion of inoculated cells, adherent cell fold expansion relates to the expansion of adherent cells, at day 1. Maximum fold expansion relates to the best cell culture day.

Seeding efficiency	Fold Expansion	Maximum Fold Expansion	Adherent Cell Fold Expansion
60%	1.54	1.69	2.56

A reduction in cell number was observed from day 2, probably due to poor cell adaptation to the increase in agitation speed from 25rpm to 50rpm. Despite this, microcarrier examination by microscopy revealed a homogeneous and monolayer occupancy of the beads with cells throughout culture (*Figure 28*). This observation suggested that the culture was facing a limitation in terms of surface area available for cell growth that at this point was about 108cm^2. For this reason, additional microcarriers with a total surface area of 72cm^2, corresponding to 66% of the initial surface area available, was added by day 5. The increase registered from day 5 afterwards indicates that cells were able to repopulate the new beads.

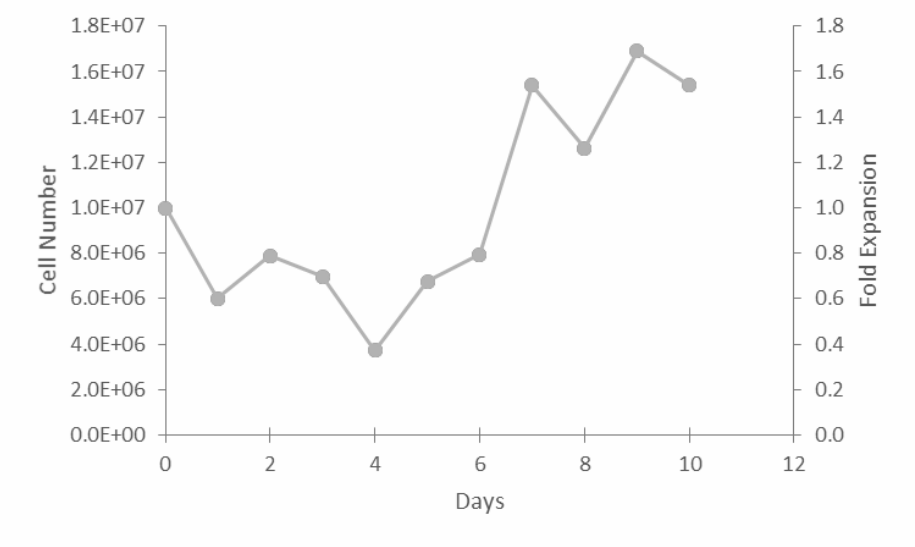

Figure 26: Growth curve of lt-NES cultured in spinner flasks with 3µg/cm^2 laminin coated plastic beads. Results of one experiment.

Cell density throughout the culture period was plotted to understand if microcarriers were confluent before the addition of the empty beads and at the end of the culture (*Figure 27)*. Cell density reduced at day 6, due to the increase in more than 50% of the available surface area, not followed by a significant increase in cell number. Probably, the number of cells inoculated was too high for the surface area available, explaining the reduced growth in the first days of culture. The new beads added in day 5 were thus rapidly populated.

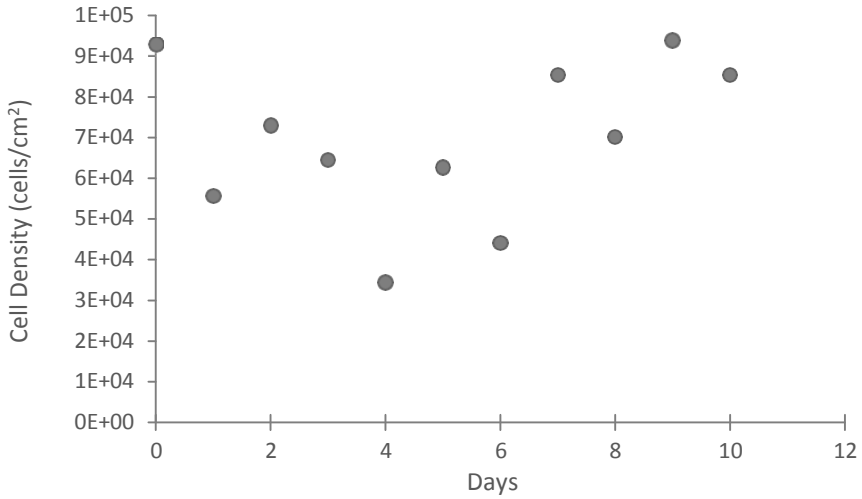

Figure 27: Cell density over time (days). Initial surface area available was 108 cm^2, increased in day 5 to 180 cm^2. Results of one experiment.

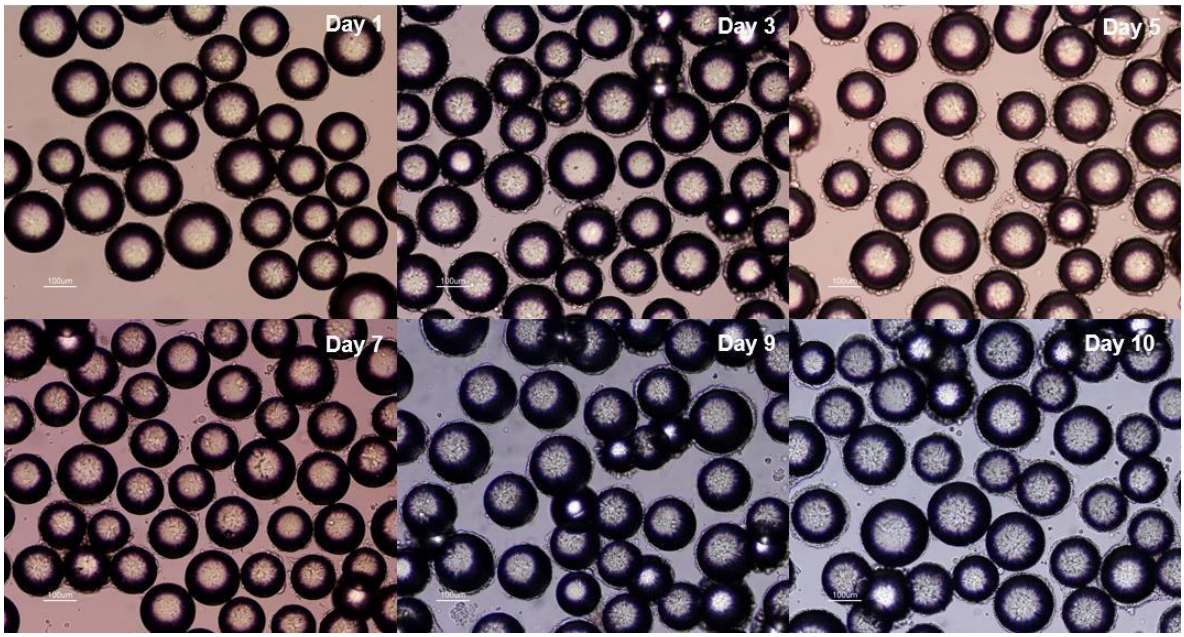

Figure 28: lt-NES cell occupancy on Plastic beads harvested in days 1, 3, 5, 7, 9 and 10 of culture in spinner flask.

In order to verify if cell culture on the poly-ornithine/laminin Plastic beads in a dynamic environment affected multipotency of the cells, the expression of neural progenitor markers Nestin, Sox2 and the neuronal differentiation marker Tuj1 was assessed by immunocytochemistry, directly on the microcarriers (*Figure 29*). Cells retained expression of Nestin and Sox2, and no detection of Tuj1 was registered. In addition, cells harvested from the microcarriers were also analyzed by immunocytochemistry for the expression of the same markers. Similar expression patterns were registered for Nestin and Sox2, while it was detected residual expression of Tuj1 (*Figure 30)*.

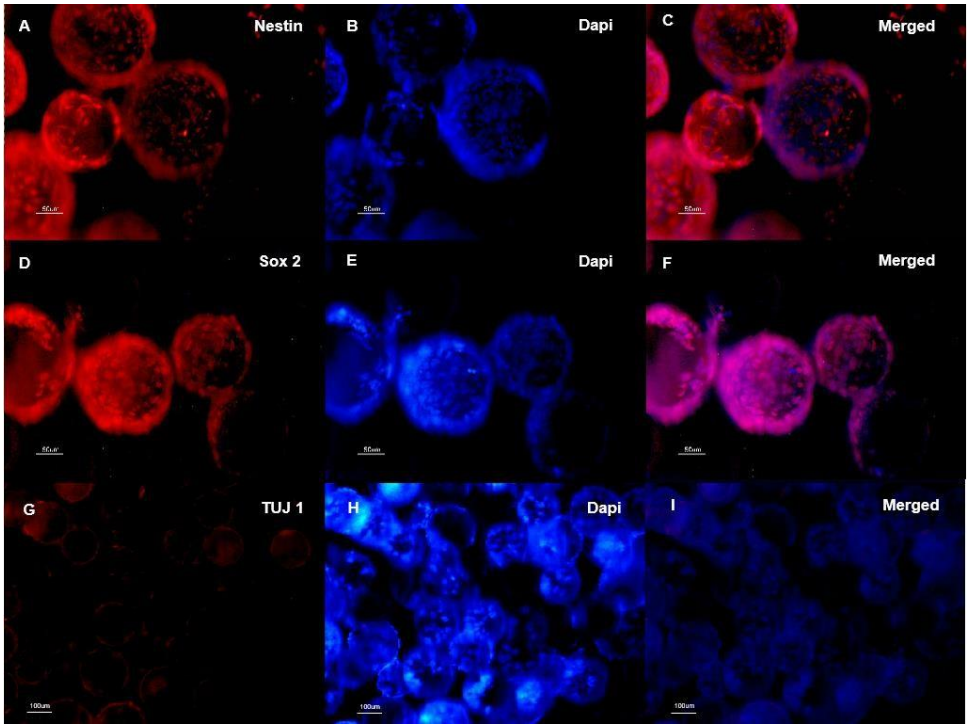

Figure 29: Immunostaining of cells for NSC markers Nestin (A-C), Sox 2 (D-F) and neuronal differentiation marker Tuj1 (G-I) expression in plastic beads cultured in spinner flasks.

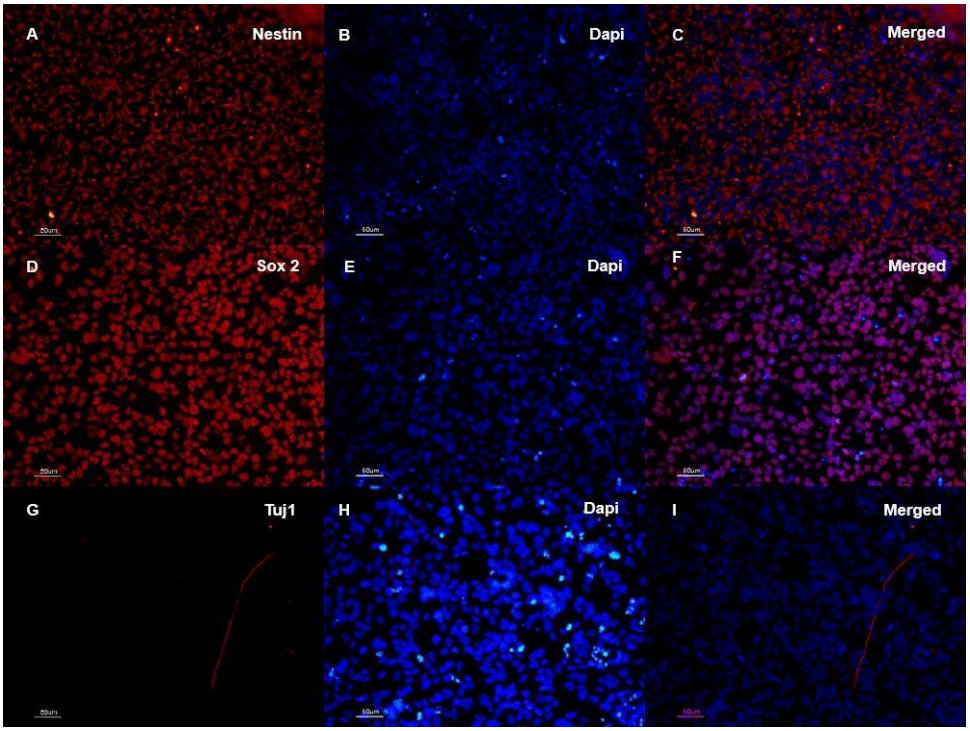

Figure 30: Immunostaining of cells harvested from plastic beads cultured in spinner flasks and replated in poly-onithine/laminin tissue culture plates. Evaluation of NSC markers Nestin (A-C), Sox 2 (D-F) and neuronal differentiation marker Tuj1(G-I) expression.

Taken together, the immunocytochemistry results indicate that lt-NES can be propagated on plastic microcarriers in a stirred environment without loss of multipotency marker expression. Confirmation of the expression of neural progenitor markers by RT-PCR would also be necessary, as well as determination of the differentiation potential of lt-NES, after culture in poly-ornithine Plastic beads in a spinner flask.

The concentration profiles of glucose and lactate throughout culture period were plotted. In *Figure 31*, no complete depletion of glucose is observed and the lower concentration detected is 14.65mM. Therefore, glucose availability was not a limiting factor for cell growth. A decrease in glucose concentration occurs until day three and slightly from day 6 until the last time point. Lactate concentrations, on the other hand, increased during the entire period, with exception of day 6. Lactate reached a maximum concentration of 17mM, which is below the growth-inhibitory concentration value for human mesenchymal stem cells (35.4mM). Specific lactate production (q_{lac}) and glucose consumption (q_{glu}) rates were calculated before and after the addition of new microcarriers to evaluate possible differences in cell metabolism which could explain the results (*Table 8)*. A higher glucose consumption rate and lactate production rate were obtained in the first stage of the culture. After the addition of beads in day 5, the average molar ratio of lactate produced over consumed glucose increased to 2.04, which indicates a less efficient glucose metabolism. The overall average molar ratio of lactate produced over consumed glucose $Y_{lac/gluc}$ was determined to be 1.69. The higher concentration of lactate in the later stages of culture led to a decrease in medium pH which in turn caused medium color transition to yellow. This is known to be detrimental for cell proliferation and may explain the lack of an exponential growth phase.

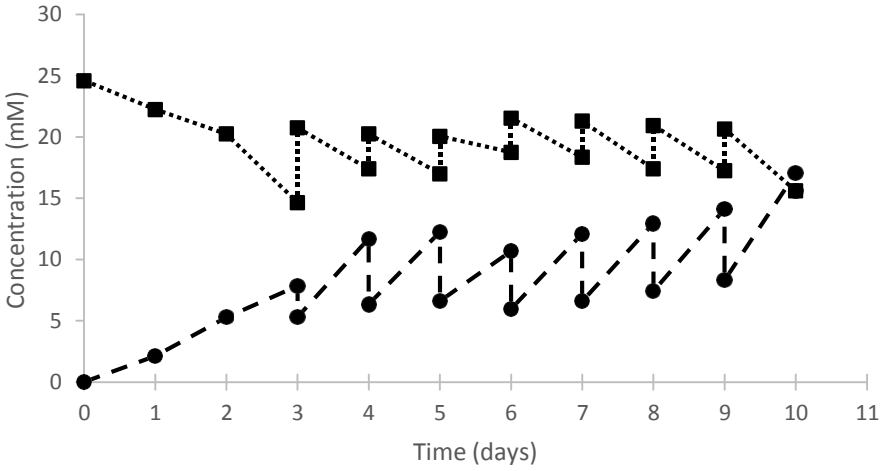

Figure 31: Concentration profile of glucose (■) and lactate (●), in mM, during lt-NES plastic beads culture in spinner flask. Results of one experiment.

Table 8: Average specific glucose consumption (q_{glu}), specific lactate production (q_{lac}) and average molar ratio of lactate produced over glucose consumption in different time periods of Plastic microcarrier in spinner flask culture.

Time period (days)	0-5	6-10	0-10
Average q_{glu} [mmol/(cell.day)]	5.17E-07	2.59E-07	3.88E-07
Average q_{lac} [mmol/(cell.day)]	6.78E-07	5.05E-07	5.91E-07
$Y_{lac/gluc}$	1.33	2.04	1.69

Based on the previous data, Plastic beads coated with poly-ornithine/ laminin, as opposed to beads with laminin covalently bound, support lt-NES cell attachment and proliferation without visible alterations in NSC phenotype. However, the culture system tested is far from being efficient and future work should focus on the optimization of initial microcarrier concentration, initial cell inoculation, agitation speed and schemes, and culture free of xenogeneic products, replacing mouse laminin for human or recombinant laminin for example, and in defined conditions, which was not the case given the use of B27. Considering cost-effective cell cultures, a profound study to determine the optimal concentration of laminin used for coating without compromising the culture performance under dynamics environments would also be valuable.

4 Conclusions

Functionalization of the microcarriers aims to provide surface cues capable of enhancing cell attachment and growth. For this purpose, laminin, an ECM protein, was conjugated to different beads either through a covalent reaction, EDC/sulfo-NHS, or physical adsorption. It was hypothesized that protein immobilization using the covalent link would be more resistant in a spinner flask culture when compared to passive coatings. Quantitation of the laminin immobilized using the Bradford assay was similar for both coupling procedures, but given the low specificity of the Bradford dye to the laminin, other methods must be considered to get conclusive remarks.

Screening of microcarriers in static environment showed that the identical coating conditions in different microcarriers does not result in similar cell expansion numbers. Cytodex 1, for example, did not exhibit remarkable results, despite the positive charges present throughout the matrix. Therefore, optimal coating parameters, for example laminin concentration, must be tested for each type of microcarrier in order to develop cost-effective scalable systems. It is also important to replicate the experiments tested to discard experimental errors.

It is also clear from this work that the results obtained with microcarrier cultures in static conditions are not directly translated to stirring environments. That was the case with –COOH beads, which supported expansion of lt-NES in tissue culture plates, however, they were inefficient in the retention of cells to the beads in spinner flasks. Since laminin covalent bonding did not result in an advantageous feature in dynamic conditions, it is proposed an additional pLL adsorption coating, which was already demonstrated in the literature to be successful in the cultivation of hPSCs in stirred suspensions vessels [58]. It is also of great importance to evaluate different agitation schemes and speeds to prevent cell detachment.

Poly-ornithine/laminin Plastic microcarriers yielded the most promising results for the proliferation of lt-NES cells in spinner flask. After 9 days in culture, a maximum 1.69 fold increase in cell number was registered, and maintenance of the neural stem/progenitor markers, such as Nestin and Sox2, was confirmed by immunocytochemistry. Despite the reduction in cell growth in the first days of culture, homogeneous and monolayer occupancy of the microcarriers was observed, which suggests that initial microcarrier concentration or initial cell density are candidate parameters for optimization. Furthermore, this culture system was not performed in defined conditions, given the use of medium supplement B27, whose formulation is not known. Xeno-derived products must also be discarded or replaced, since are sources of variability and contamination. For instance, mouse laminin could be replaced by human laminin, however, the high costs associated to the production of laminin from such a source would hinder the scale-up of this system. In addition, further characterization of the dynamically expanded cells would be necessary to validate culture using Plastic microcarriers in stirred vessels. Additional work should include an analysis to the gene expression of specific markers by RT-PCR and to differentiation potential,

by induction of differentiation into neurons and glia, to confirm phenotypic and stemness properties, respectively. Controlling lactate production to prevent acidification of the medium, by monitoring culture pH could be achieved through operation under perfusion or by adding a basic solution.

In future work, it would also be interesting to study biodegradable microcarriers in the culture of lt-NES, such as gelatin or alginate, given the ease of separation of cells from the beads while theoretically providing a more safe environment by preventing the aggressive action of enzymatic disaggregation and reducing the costs. Other types of bioreactor configurations, for example, rotary wall vessels, or with different types of impellers, may be used to minimize the shear forces exerted over the cells.

Considerable progress is still required before NSCs potential can be fully exploited in cell therapy, drug discovery or disease modeling. Native NSCs microarchitecture, interactions with neighboring cells and exposure to biochemical signals, must be extensively explored so researchers could better mimic *in vitro* the neurogenic niches, with the purpose of providing a suitable and safe environment for cell attachment and proliferation. Simultaneously, development of cost-effective and reproducible systems is of key importance for the production of the large number of cells required for biomedical applications.

5 References

1. Sanders, R.C., Jr., et al., *Stem cell research.* Paediatr Respir Rev, 2006. **7**(2): p. 135-40.
2. Bongso, A. and E.H. Lee, *Stem Cells: From Bench to Bedside*. 2005: World Scientific.
3. Thomson, J.A., et al., *Embryonic stem cell lines derived from human blastocysts.* Science, 1998. **282**(5391): p. 1145-7.
4. Takahashi, K. and S. Yamanaka, *Induction of pluripotent stem cells from mouse embryonic and adult fibroblast cultures by defined factors.* Cell, 2006. **126**(4): p. 663-76.
5. Takahashi, K., et al., *Induction of pluripotent stem cells from adult human fibroblasts by defined factors.* Cell, 2007. **131**(5): p. 861-72.
6. Lowry, W.E. and W.L. Quan, *Roadblocks en route to the clinical application of induced pluripotent stem cells.* J Cell Sci, 2010. **123**(Pt 5): p. 643-51.
7. Conti, L. and E. Cattaneo, *Neural stem cell systems: physiological players or in vitro entities?* Nat Rev Neurosci, 2010. **11**(3): p. 176-87.
8. Gorba, T. and L. Conti, *Neural stem cells as tools for drug discovery: novel platforms and approaches.* Expert Opin Drug Discov, 2013. **8**(9): p. 1083-94.
9. Bergstrom, T. and K. Forsberg-Nilsson, *Neural stem cells: brain building blocks and beyond.* Ups J Med Sci, 2012. **117**(2): p. 132-42.
10. Malatesta, P., I. Appolloni, and F. Calzolari, *Radial glia and neural stem cells.* Cell Tissue Res, 2008. **331**(1): p. 165-78.
11. Barry, D.S., J.M. Pakan, and K.W. McDermott, *Radial glial cells: key organisers in CNS development.* Int J Biochem Cell Biol, 2014. **46**: p. 76-9.
12. Gotz, M. and W.B. Huttner, *The cell biology of neurogenesis.* Nat Rev Mol Cell Biol, 2005. **6**(10): p. 777-88.
13. Crews, F.T. and K. Nixon, *Alcohol, neural stem cells, and adult neurogenesis.* Alcohol Res Health, 2003. **27**(2): p. 197-204.
14. Erceg, S., M. Ronaghi, and M. Stojkovic, *Human embryonic stem cell differentiation toward regional specific neural precursors.* Stem Cells, 2009. **27**(1): p. 78-87.
15. Atala, A. and R. Lanza, *Handbook of Stem Cells*. 2012: Academic Press.
16. Falk, A., et al., *Capture of neuroepithelial-like stem cells from pluripotent stem cells provides a versatile system for in vitro production of human neurons.* PLoS One, 2012. **7**(1): p. e29597.
17. Koch, P., et al., *A rosette-type, self-renewing human ES cell-derived neural stem cell with potential for in vitro instruction and synaptic integration.* Proc Natl Acad Sci U S A, 2009. **106**(9): p. 3225-30.
18. Jensen, J.B. and M. Parmar, *Strengths and limitations of the neurosphere culture system.* Mol Neurobiol, 2006. **34**(3): p. 153-61.
19. Conti, L., et al., *Niche-independent symmetrical self-renewal of a mammalian tissue stem cell.* PLoS Biol, 2005. **3**(9): p. e283.
20. Pollard, S.M., et al., *Adherent neural stem (NS) cells from fetal and adult forebrain.* Cereb Cortex, 2006. **16 Suppl 1**: p. i112-20.
21. Ferreira, I.A.F., *Biofunctionalization of electrospun poly(epslon-caprolactone) nanofibers to promote neural stem cell adhesion, alignment and expansion*. 2013, Instituto Superior Técnico, Universidade Técnica de Lisboa.
22. Gage, F.H., et al., *Survival and differentiation of adult neuronal progenitor cells transplanted to the adult brain.* Proc Natl Acad Sci U S A, 1995. **92**(25): p. 11879-83.

23. Wakeman, D.R., et al., *Human neural stem cells survive long term in the midbrain of dopamine-depleted monkeys after GDNF overexpression and project neurites toward an appropriate target.* Stem Cells Transl Med, 2014. **3**(6): p. 692-701.
24. Englund, U., et al., *Transplantation of human neural progenitor cells into the neonatal rat brain: extensive migration and differentiation with long-distance axonal projections.* Exp Neurol, 2002. **173**(1): p. 1-21.
25. Wennersten, A., et al., *Proliferation, migration, and differentiation of human neural stem/progenitor cells after transplantation into a rat model of traumatic brain injury.* J Neurosurg, 2004. **100**(1): p. 88-96.
26. Ahmed, S., *The culture of neural stem cells.* J Cell Biochem, 2009. **106**(1): p. 1-6.
27. Gage, F.H. and S. Temple, *Neural stem cells: generating and regenerating the brain.* Neuron, 2013. **80**(3): p. 588-601.
28. Lancaster, M.A., et al., *Cerebral organoids model human brain development and microcephaly.* Nature, 2013. **501**(7467): p. 373-9.
29. Payne, N.L., et al., *Application of human induced pluripotent stem cells for modeling and treating neurodegenerative diseases.* N Biotechnol, 2015. **32**(1): p. 212-28.
30. Fernandes, T.G., et al., *Neural commitment of human pluripotent stem cells under defined conditions recapitulates neural development and generates patient-specific neural cells.* Biotechnol J, 2015. **10**(10): p. 1578-88.
31. Rodrigues, C.A., et al., *Stem cell cultivation in bioreactors.* Biotechnol Adv, 2011. **29**(6): p. 815-29.
32. Tandon, N., et al., *Bioreactor engineering of stem cell environments.* Biotechnol Adv, 2013. **31**(7): p. 1020-31.
33. Serra, M., et al., *Process engineering of human pluripotent stem cells for clinical application.* Trends Biotechnol, 2012. **30**(6): p. 350-9.
34. Placzek, M.R., et al., *Stem cell bioprocessing: fundamentals and principles.* J R Soc Interface, 2009. **6**(32): p. 209-32.
35. *StemCell Technologies website, http://www.stemcell.com/en/Products/All-Products/StemSpan-Spinner-Flask.aspx, last accessed on October 2015*.
36. Cabrita, G.J., et al., *Hematopoietic stem cells: from the bone to the bioreactor.* Trends Biotechnol, 2003. **21**(5): p. 233-40.
37. Scientific, T., *Protein Assay Technical Handbook*.
38. Gibson, C., *Development of novel microcarriers for adipose derived stem cell material directed differentiation and expansion*. 2012, Cardiff University: Cardiff School of Biosciences.
39. Barzegari, A. and A.A. Saei, *An update to space biomedical research: tissue engineering in microgravity bioreactors.* Bioimpacts, 2012. **2**(1): p. 23-32.
40. *Proceedings of the Production of Monoclonal Antibodies Workshop*. 1999. Bologna, Italy.
41. *GE Healthcare Life Sciences website, http://www.gelifesciences.com/webapp/wcs/stores/servlet/catalog/en/GELifeSciences-pt/brands/wave/, last accessed on October 2015*.
42. Serra, M., et al., *Improving expansion of pluripotent human embryonic stem cells in perfused bioreactors through oxygen control.* J Biotechnol, 2010. **148**(4): p. 208-15.
43. Rodrigues, C.A., et al., *Microcarrier expansion of mouse embryonic stem cell-derived neural stem cells in stirred bioreactors.* Biotechnol Appl Biochem, 2011. **58**(4): p. 231-42.
44. Hillberg, A.L., et al., *Improving alginate-poly-L-ornithine-alginate capsule biocompatibility through genipin crosslinking.* J Biomed Mater Res B Appl Biomater, 2013. **101**(2): p. 258-68.
45. van Wezel, A.L., *Growth of cell-strains and primary cells on micro-carriers in homogeneous culture.* Nature, 1967. **216**(5110): p. 64-5.

46. Malda, J. and C.G. Frondoza, *Microcarriers in the engineering of cartilage and bone.* Trends Biotechnol, 2006. **24**(7): p. 299-304.
47. Guanghui Ma, Z.S., *Microspheres and microcapsules in biotechnology: design, preparation and applications*. 2013: CRC Press. 552.
48. Chen, A.K., et al., *Critical microcarrier properties affecting the expansion of undifferentiated human embryonic stem cells.* Stem Cell Res, 2011. **7**(2): p. 97-111.
49. Sciences, G.H.L., *Microcarrier Cell Culture: Principles and Methods*, in *Handbook*, G.H.L. Sciences, Editor. 2013.
50. John Rowley, E.A., Andrew Campbell, Harvey Brandwein, Steve Oh, *Meeting lot-size challenges of manufacturing adherent cells for therapy.* BioProcess International, 2012. **10**(3): p. 16-22.
51. Hjortso, M.A. and J.W. Roos, *Cell adhesion : fundamentals and biotechnological applications*. Bioprocess technology. 1995, New York: M. Dekker. xi, 273 p.
52. Little, L., K.E. Healy, and D. Schaffer, *Engineering biomaterials for synthetic neural stem cell microenvironments.* Chem Rev, 2008. **108**(5): p. 1787-96.
53. Sun, Y., et al., *Mechanics regulates fate decisions of human embryonic stem cells.* PLoS One, 2012. **7**(5): p. e37178.
54. Laleh Ghasemi-Mobarakeh, M.P.P., Mohammad Morshed, Mohammad Hossein Nasr-Esfahani, S. Ramakrishna, *Bio-functionalized PCL nanofibrous scaffolds for nerve tissue engineering.* Materials Science and Engineering: C, 2010. **30**(8): p. 1129-1136.
55. Oh, S.K., et al., *Long-term microcarrier suspension cultures of human embryonic stem cells.* Stem Cell Res, 2009. **2**(3): p. 219-30.
56. Nie, Y., et al., *Scalable culture and cryopreservation of human embryonic stem cells on microcarriers.* Biotechnol Prog, 2009. **25**(1): p. 20-31.
57. Bertolo, A., et al., *Growth Factors Cross-Linked to Collagen Microcarriers Promote Expansion and Chondrogenic Differentiation of Human Mesenchymal Stem Cells.* Tissue Eng Part A, 2015.
58. Fan, Y., et al., *Facile engineering of xeno-free microcarriers for the scalable cultivation of human pluripotent stem cells in stirred suspension.* Tissue Eng Part A, 2014. **20**(3-4): p. 588-99.
59. Santiago, L.Y., et al., *Peptide-surface modification of poly(caprolactone) with laminin-derived sequences for adipose-derived stem cell applications.* Biomaterials, 2006. **27**(15): p. 2962-9.
60. Zhu, Y., et al., *Surface modification of polycaprolactone membrane via aminolysis and biomacromolecule immobilization for promoting cytocompatibility of human endothelial cells.* Biomacromolecules, 2002. **3**(6): p. 1312-9.
61. Hermanson, G.T., *Bioconjugate techniques*. 2nd ed. ed. 2008, London: Academic.
62. Grabarek, Z. and J. Gergely, *Zero-length crosslinking procedure with the use of active esters.* Anal Biochem, 1990. **185**(1): p. 131-5.
63. Scientific, T., *Crosslinking Technical Handbook*.
64. Villa-Diaz, L.G., et al., *Concise review: The evolution of human pluripotent stem cell culture: from feeder cells to synthetic coatings.* Stem Cells, 2013. **31**(1): p. 1-7.
65. Beck, K., I. Hunter, and J. Engel, *Structure and function of laminin: anatomy of a multidomain glycoprotein.* FASEB J, 1990. **4**(2): p. 148-60.
66. Brafman, D.A., et al., *Long-term human pluripotent stem cell self-renewal on synthetic polymer surfaces.* Biomaterials, 2010. **31**(34): p. 9135-44.
67. Kallos, M.S. and L.A. Behie, *Inoculation and growth conditions for high-cell-density expansion of mammalian neural stem cells in suspension bioreactors.* Biotechnol Bioeng, 1999. **63**(4): p. 473-83.
68. Kallos, M.S., A. Sen, and L.A. Behie, *Large-scale expansion of mammalian neural stem cells: a review.* Med Biol Eng Comput, 2003. **41**(3): p. 271-82.

69. Gilbertson, J.A., et al., *Scaled-up production of mammalian neural precursor cell aggregates in computer-controlled suspension bioreactors.* Biotechnol Bioeng, 2006. **94**(4): p. 783-92.
70. Lin, H.J., et al., *Neural stem cell differentiation in a cell-collagen-bioreactor culture system.* Brain Res Dev Brain Res, 2004. **153**(2): p. 163-73.
71. Rodrigues, C.A.V., *Design and operation of bioreactor systems for the expansion and controlled differentiation of stem cells*. 2011, Universidade Técnica de Lisboa: Instituto Superior Técnico. p. 170.
72. Baghbaderani, B.A., et al., *Bioreactor expansion of human neural precursor cells in serum-free media retains neurogenic potential.* Biotechnol Bioeng, 2010. **105**(4): p. 823-33.
73. *Protocol for EDC/sulfo-NHS crosslinking, Thermo Fisher Scientific website, https://tools.thermofisher.com/content/sfs/manuals/MAN0011309_NHS_SulfoNHS_UG.pdf, last accessed on October 2015*.
74. Bradford, M.M., *A rapid and sensitive method for the quantitation of microgram quantities of protein utilizing the principle of protein-dye binding.* Anal Biochem, 1976. **72**: p. 248-54.
75. *User Guide: Coomassie Plus (Bradford) Assay Kit, Thermo Fisher Scientific website, https://tools.thermofisher.com/content/sfs/manuals/MAN0011203_CoomassiePlus_Bradford_Asy_UG.pdf, last accessed on October 2015.*
76. Junka, R., et al., *Laminin Functionalized Biomimetic Nanofibers For Nerve Tissue Engineering.* J Biomater Tissue Eng, 2013. **3**(4): p. 494-502.
77. Read, S.M. and D.H. Northcote, *Minimization of variation in the response to different proteins of the Coomassie blue G dye-binding assay for protein.* Anal Biochem, 1981. **116**(1): p. 53-64.
78. Dame, M.K. and J. Varani, *Recombinant collagen for animal product-free dextran microcarriers.* In Vitro Cell Dev Biol Anim, 2008. **44**(10): p. 407-14.
79. Alves, P., et al., *Surface grafting of a thermoplastic polyurethane with methacrylic acid by previous plasma surface activation and by ultraviolet irradiation to reduce cell adhesion.* Colloids Surf B Biointerfaces, 2011. **82**(2): p. 371-7.
80. Alfred, R., et al., *Efficient suspension bioreactor expansion of murine embryonic stem cells on microcarriers in serum-free medium.* Biotechnol Prog, 2011. **27**(3): p. 811-23.
81. Schop, D.J., Frank W.; van Rijn, Linda D.S.;Fernandes, Hugo; Rolf M. Bloem, Joost D. de Bruijn, and Riemke van Dijkhuizen-Radersma, *Growth, Metabolism, and Growth Inhibitors of Mesenchymal Stem Cells* Tissue Engineering Part A, 2009. **15**(8): p. 1877-1886.
82. Schop, D., et al., *Expansion of human mesenchymal stromal cells on microcarriers: growth and metabolism.* J Tissue Eng Regen Med, 2010. **4**(2): p. 131-40.